Targeting Siglecs with a sialic acid-decorated nanoparticle abrogates inflammation

Spence, S., Greene, M. K., Fay, F., Hams, E., Saunders, S. P., Hamid, U., Fitzgerald, M., Beck, J., Bains, B. K., Smyth, P., Themistou, E., Small, D. M., Schmid, D., O'Kane, C. M., Fitzgerald, D. C., Abdelghany, S. M., Johnston, J. A., Fallon, P. G., Burrows, J. F., ... Scott, C. J. (2015). Targeting Siglecs with a sialic acid-decorated nanoparticle abrogates inflammation. *Science Translational Medicine*, *7*(303), [140]. https://doi.org/10.1126/scitranslmed.aab3459

Published in:
Science Translational Medicine

Document Version:
Peer reviewed version

Title: Targeting Siglecs with a sialic acid-decorated nanoparticle abrogates inflammation

Authors: S. Spence[1*], M. K. Greene[2*], F. Fay[2,3], E. Hams[4], S. P. Saunders[4], U. Hamid[1], M. Fitzgerald[1], J. Beck[1], B. K. Bains[2], P. Smyth[2], E. Themistou[5], D. M. Small[1], D. Schmid[2], C. M. O'Kane[1], D. Fitzgerald[1], S. M. Abdelghany[2,6], J. A. Johnston[1,7], P. G. Fallon[4,8], J. F. Burrows[2], D. F. McAuley[1], A. Kissenpfennig[1], C. J. Scott[2‡]

[*]These authors contributed equally

Affiliations:

[1]Centre for Infection and Immunity, School of Medicine, Dentistry and Biomedical Sciences, Queen's University Belfast, Belfast, UK

[2]School of Pharmacy, Queen's University Belfast, Belfast, UK

[3]Translational and Molecular Imaging Institute, Icahn School of Medicine at Mount Sinai, New York, USA

[4]Trinity Biomedical Sciences Institute, School of Medicine, Trinity College Dublin, Dublin, Ireland

[5]School of Chemistry and Chemical Engineering, Queen's University Belfast, Belfast, UK

[6]Faculty of Pharmacy, The University of Jordan, Amman, Jordan

[7]Inflammation Research, Amgen Inc., Thousand Oaks, USA

[8]National Children's Research Centre, Our Lady's Children's Hospital, Dublin, Ireland

[‡]**Corresponding Author:**

Christopher Scott

Molecular Therapeutics

School of Pharmacy

Queens University Belfast

97 Lisburn Road

Belfast, UK

BT9 7BL

Email: c.scott@qub.ac.uk

Tel: +44(0)2890972350

Fax: +44(0)2890977794

One sentence summary:

Siglec receptor activation by a nanoparticle functionalized with sialic acid reduces macrophage-driven inflammation via an IL-10 dependent mechanism.

Abstract:

Sepsis is the single most frequent cause of death in hospitalized patients and severe sepsis is a leading contributory factor to Acute Respiratory Distress Syndrome (ARDS). At present there is no effective treatment for these conditions and care is primarily supportive. Murine sialic acid-binding immunoglobulin-like lectin-E (Siglec-E) and its human orthologs Siglec-7 and -9 are immunomodulatory receptors found predominantly on hematopoietic cells. These receptors are important negative regulators of acute inflammatory responses and are potential targets for the treatment of sepsis and ARDS. In this study, we describe a Siglec targeting platform consisting of poly(lactic-co-glycolic acid) (PLGA) nanoparticles decorated with a natural Siglec ligand: di(α2→8) N-acetylneuraminic acid (α2,8 NANA-NP). This nanoparticle induced enhanced oligomerization of the murine Siglec-E receptor on the surface of macrophages, unlike the free α2,8 NANA ligand. Furthermore, treatment of murine macrophages with these nanoparticles blocked the production of lipopolysaccharide (LPS)-induced inflammatory cytokines in a Siglec-E dependent manner. The nanoparticles were also therapeutically beneficial in vivo in both systemic and pulmonary murine models of inflammation. Moreover, we confirmed the anti-inflammatory effect of these nanoparticles on human monocytes and macrophages in vitro and in an ex vivo lung perfusion (EVLP) model of lung injury. We also established that IL-10 induced Siglec-E expression, and α2,8 NANA-NP augmented the expression of IL-10 further. Indeed, the effectiveness of the nanoparticle depended on IL-10. Collectively, these results demonstrated a therapeutic effect by targeting Siglec receptors in inflammatory conditions with a nanoparticle-based platform.

Introduction:

Sepsis is the single most frequent cause of death in hospitalized patients. Recent statistics have estimated occurrence worldwide as higher than 19 million cases per year. Unfortunately, despite 8 million sepsis-caused deaths annually, there is no effective treatment. Current treatments are supportive, and often ineffective, with survivors tending to show persistent critical illness (PCI), which presents as long-term organ dysfunction (1, 2). In addition, approximately 25% of patients with severe sepsis progress to develop Acute Respiratory Distress Syndrome (ARDS) (3) and mortality from ARDS is approximately 25-30% (4). The excessive pro-inflammatory responses that contribute to organ dysfunction in sepsis are typically initiated and driven by the Toll-like receptors (TLRs), which recognize pathogen-derived constituents such as lipopolysaccharide (LPS), bacterial lipoproteins and non-methylated CpG DNA (5). Additionally, TLRs signal sterile inflammatory responses driven by damage-associated molecular patterns (DAMPs).

Sialic acid-binding immunoglobulin-like lectins (Siglecs) were originally identified as cell-surface transmembrane receptors found primarily on hematopoietic cells and are capable of inhibiting TLR signaling (6). Hence, Siglecs have attracted attention as diagnostic and therapeutic biomarkers in various diseases including acute myeloid leukemia, lymphoma, rheumatological disease and allergy (7-9). One member of this family, Siglec-E (and its human orthologues Siglec-7 and -9) is predominantly found on macrophages and neutrophils. Siglec-E is an important regulator of neutrophil infiltration during pulmonary inflammation (10) and is capable of abrogating TLR-mediated responses through tyrosine specific Src homology-2 domain-containing phosphatase-2 (SHP-2) recruitment (11). Likewise, the human ortholog Siglec-7 is present on various immune cell subsets and recruits SHP-1 upon activation to downregulate inflammatory mediators (12, 13).

The natural ligands for Siglecs are sialic acids, which are derivatives of N-acetylneuraminic acid (NANA), a monosaccharide with a nine-carbon backbone that can be linked to other sugars generating considerable diversity (14). Importantly, sialic acids act as signaling molecules, activating Siglecs expressed on the surface of immune cells both in cis and in trans to initiate inhibitory signal transduction. Recognition of sialic acids by the Siglecs is particularly dependent on the point-to-point saccharide linkage ($\alpha2\rightarrow3$, $\alpha2\rightarrow6$ and $\alpha2\rightarrow8$) with different Siglec receptors having various binding preferences (15). We therefore have examined the therapeutic potential of targeting Siglecs in models of acute inflammation. Previous studies by ourselves (16) and others (17) have utilized complexed antibody strategies to engage Siglec receptors. However, the ability of bivalent antibodies to oligomerize receptors in vivo translates poorly to

patients (18). As an alternative approach, we here specifically target and activate Siglec receptors using a sialylated nanoparticle.

Results:

α2,8 NANA-NP target Siglec-E on macrophages to limit LPS-driven pro-inflammatory cytokine production in vitro.

Biodegradable and biocompatible 150-nm poly(lactic-co-glycolic acid) (PLGA) nanoparticles were prepared with a salting out formulation method (19) and decorated with α2,8 NANA (α2,8 NANA-NP), prior to physicochemical characterization (Fig. S1). The capacity of α2,8 NANA-NP to elicit anti-inflammatory effects was then evaluated in peritoneal macrophages stimulated for 12hr with LPS ± α2,8 NANA-NP or associated controls. Exposure of macrophages to α2,8 NANA-NP significantly attenuated LPS-induced production of the pro-inflammatory cytokines TNF-α and IL-6 (Fig. 1A and 1B). These reductions were specifically attributed to the surface-display of α2,8 NANA because a series of controls did not produce similar anti-inflammatory effects: These included free α2,8 NANA alone, non-functionalized nanoparticles (Nude-NP) or nanoparticles decorated with glucosamine (Glucosamine NP). Furthermore, the anti-inflammatory effects depended on both the dose and on surface density of α2,8 NANA, with increasing sialic acid concentrations [1.4 to 15 μg] eliciting greater inhibitory effects. Moreover, the inhibitory effects of a single treatment of α2,8 NANA-NP were maintained for 24 hr, with minimal batch-to-batch variation (Fig. S1).

Subsequently, we examined the specificity of the nanoparticle towards Siglec-E. Treatment of peritoneal macrophages with LPS induced Siglec-E mRNA and protein levels (Fig. 1C and 1D). LPS induction of Siglec-E was also shown in bone marrow-derived macrophages (BMDM) (Fig. 1E). Having demonstrated the presence of Siglec-E on LPS-stimulated macrophages, we sought to confirm that receptor engagement was required for the anti-inflammatory effects of these nanoparticles. In an initial experiment, we showed enhanced binding of α2,8 NANA-NP to recombinant Siglec-E Fc protein in vitro over non-functionalized control nanoparticles (Fig. S2). Next, the effects of the nanoparticles were determined in cells where surface Siglec-E had been pre-blocked with a non-agonistic antibody. This receptor blocking significantly impeded the anti-inflammatory capacity of α2,8 NANA-NP compared to controls (Fig. 1F). In order to conclusively rule out antibody cross-linking effects, Siglec-E was depleted in cells with RNA interference. Depletion of Siglec-E mRNA ablated the anti-inflammatory effects of α2,8 NANA-NP (Fig. 1G). The specificity of α2,8 NANA-NP for Siglec-E was further demonstrated by microscopy studies, in which increased adherence of the nanoparticle to macrophages was observed, upon surface-decoration with α2,8

NANA (Fig. 1H). This preferential binding of α2,8 NANA-NP was markedly reduced by pre-blocking with Siglec-E antibody (Fig. 1I). Finally, we investigated the clustering of Siglec-E on the plasma membrane of macrophages with fluorescent α2,8 NANA-NP (Fig. S2). Siglec-E localization was enhanced at areas of high α2,8 NANA-NP density compared with Nude-NP or Siglec-E non-agonistic antibody controls. This clustering was indicative of increased receptor activation (20, 21). Collectively, these data demonstrate that the anti-inflammatory effects of α2,8 NANA-NP towards murine macrophages occur via enhanced interactions with Siglec-E molecules, and are Siglec-E dependent.

α2,8 NANA-NP attenuate inflammatory effects in murine models of systemic inflammation.

The therapeutic potential of α2,8 NANA-NP in vivo was next examined in a mouse model of LPS-induced systemic inflammation. Mice were challenged with an intraperitoneal (i.p.) injection of a lethal dose of LPS (6mg/kg) and treated with either α2,8 NANA-NP or Nude-NP i.p. at 0hr. In this lethal model 7/8 animals treated with Nude-NP reached experimental endpoint within 32hr, while animals treated with α2,8 NANA-NP remained healthy (Fig. 2A). The survival benefits conferred by α2,8 NANA-NP corresponded with a significant reduction in serum TNF-α (Fig. 2B) and increased levels of IL-10 (Fig. 2C). Having demonstrated that α2,8 NANA-NP could prophylactically prevent death in LPS-induced systemic inflammation, we next examined efficacy after the onset of inflammation (defined as a clinical score of 2: piloerection, huddling and diarrhea). α2,8 NANA-NP (2mg) or controls were administered at the peak of inflammation (2hr post-LPS), in accordance with previous reports (22). Similar to prophylactic treatment, α2,8 NANA-NP significantly enhanced survival (Fig. 2D) and analogous attenuation of serum TNF-α (Fig. 2E) and elevated IL-10 (Fig. 2F) were observed.

As recent reports had indicated that Siglec-E was present on other innate immune cells, particularly neutrophils (10), we questioned whether the therapeutic effects of α2,8 NANA-NP were solely macrophage dependent in vivo. Therefore, mice were treated i.p. with clodronate liposomes to deplete macrophages (Fig. S3) (23) prior to administration of LPS and nanoparticles. No abnormal clinical signs were observed subsequent to depletion. However, the therapeutic benefit of α2,8 NANA-NP was lost in macrophage-depleted mice, with no significant difference in survival observed between Nude-NP and α2,8 NANA-NP groups (Fig. 2G). We also examined the binding of α2,8 NANA-NP to cell populations in peritoneal exudate. We observed that both macrophages ($CD11b^+F4/80^+$) and neutrophils ($CD11b^+Ly6G^+$) were Siglec-E-positive, although relative expression was greater on macrophages. This was reflected in greater binding of α2,8 NANA-NP by macrophages, whilst neutrophil binding was

negligible (Fig. S4). Taken together, these results indicated that α2,8 NANA-NP-mediated effects in vivo were a consequence of binding to Siglec-E expressed on macrophages.

Thus far, the validation of α2,8 NANA-NP as a viable therapy was solely based on experimental models with LPS-driven inflammation. Therefore, the nanoparticles were next evaluated in the caecal ligation and puncture (CLP) model of polymicrobial sepsis. Inflammation in this model is driven by a multitude of TLR ligands and is much more clinically representative of sepsis and other acute inflammatory disorders (24, 25). Mice were anesthetized and CLP was performed as described previously (25). At 2hr post-surgery and every 24hr subsequently, mice were treated with α2,8 NANA-NP, Nude-NP or associated controls. α2,8 NANA-NP markedly prolonged survival, while all other control animals failed to survive beyond 8 days (Fig. 2H). Moreover, while all groups initially developed clinical signs of sepsis, α2,8 NANA-NP attenuated further progression of illness from day 2 onwards (Fig. 2I). These findings were also supported by core body temperature stabilization compared to controls (Fig. 2J). Collectively, these data suggest that α2,8 NANA-NP can produce therapeutic effects in a clinically relevant model of inflammation.

α2,8 NANA-NP attenuate inflammatory effects in murine models of lung injury.

Having established the efficacy of α2,8 NANA-NP in systemic inflammation and the CLP model of sepsis, the application of the nanoparticles in murine lung injury was next investigated. Intratracheal (i.t.) instillation of LPS in mice induces neutrophilic alveolitis and enhanced pro-inflammatory cytokine responses, features representative of the clinical features of ARDS (26-28). Following i.t. instillation of LPS, mice were administered 2mg α2,8 NANA-NP or Nude-NP i.p. 2hr post-endotoxin. Bronchoalveolar lavage (BAL) fluid neutrophilia was attenuated upon treatment with α2,8 NANA-NP, in comparison to mice that received Nude-NP (Fig. 3A). Conversely, macrophage numbers within total BAL cell populations were enhanced by α2,8 NANA-NP (Fig. 3B). Cytokine analyses also revealed that IL-10 levels were significantly elevated following α2,8 NANA-NP administration (Fig. 3C).

CLP has previously been employed to model pulmonary inflammation as a consequence of a systemic insult (29, 30). Therefore, the therapeutic efficacy of α2,8 NANA-NP was investigated in this indirect model of lung injury. At 6-8hr post-CLP, mice were treated i.t. with 20μg α2,8 NANA-NP or Nude-NP. Clinical scores were significantly lower after treatment with α2,8 NANA-NP (Fig. 3D), leading to a reduced mortality rate (Fig. 3E). These findings were consistent with the observed reductions in BAL fluid total cell counts (Fig. 3F) and neutrophil numbers (Fig. 3G). Collectively, these data suggest that α2,8

NANA-NP represent a viable therapeutic in murine models of lung injury using both i.p. and i.t. administration routes.

IL-10 induced Siglec-E upregulation is potentiated by α2,8 NANA-NP.

We next examined the mode of action of these potent anti-inflammatory nanoparticles. In previous murine studies, SHP-2 was recruited to the cytoplasmic domains of Siglec-E after receptor activation (11). Increased amounts of immunoprecipitated SHP-2 bound to Siglec-E were confirmed in cells treated with α2,8 NANA-NP, in comparison to Nude-NP-treated controls (lanes 4-6 vs. 7-9) (Figure 4A). Indicative of an anti-inflammatory response, α2,8 NANA-NP elevated Nuclear Factor Kappa B (NFκB) p50:p65 ratio within the nucleus (Fig. 4B). A key observation from our earlier data was that serum IL-10 was elevated in mice treated with α2,8 NANA-NP (Fig. 2C and 2F). However, the ability of α2,8 NANA-NP to enhance production of IL-10 was ablated in the absence of myeloid differentiation primary response gene 88 (MyD88) (Fig. 4C) confirming previous reports that MyD88 was required for LPS-stimulated IL-10 production (Fig. 4D) (31).

Previous studies had indicated that Siglec-E expression is dependent upon MyD88 function (11). Therefore, we examined expression of Siglec-E induced by both LPS and IL-10 in more detail. Similar upregulation of both Siglec-E mRNA and protein was confirmed in peritoneal macrophages treated with either stimulus (Fig. 5A and 5B). In parallel studies, pre-blocking the IL-10 receptor resulted in marked ablation of Siglec-E levels on treatment with either LPS or IL-10 (Fig. 5C). Taken together, these data demonstrated that IL-10 regulated the expression of Siglec-E. We hypothesized that the effect of the nanoparticles would therefore be dependent on IL-10. This was confirmed using IL-$10^{-/-}$ mice, where administration of α2,8 NANA-NP was unable to rescue these animals from LPS-induced mortality (Fig. 5D), nor reduce serum TNF-α in comparison to WT controls (Fig. 5E).

α2,8 NANA-NP exhibit negligible toxicity in pre-clinical models.

To analyze possible side-effects of α2,8 NANA-NP, we also assessed indicators of toxicity. To mimic the treatment regime of Fig. 2, mice were treated with a single i.p. dose of α2,8 NANA-NP or PBS. We saw no alterations in lung, liver or kidney histology among groups. Furthermore, α2,8 NANA-NP did not alter serum LDH concentrations nor animal weights. Similarly no toxic effects were observed after weekly i.p. administration of α2,8 NANA-NP over 28 days, or in a bolus localized pulmonary delivery model (Fig. S5).

α2,8 NANA-NP elicit anti-inflammatory effects in human cell and whole lung ex vivo perfusion models.

The translational potential of the nanoparticle was next explored in human models. Siglec-7 and -9 are the human orthologs of murine Siglec-E and represent translational targets for α2,8 NANA-NP. Flow cytometry analyses revealed that both receptors were present on primary human monocyte-derived macrophages (MDM) (Fig. 6A) and monocytes (Fig. 6F). Treatment of MDM with α2,8 NANA-NP significantly attenuated LPS-induced secretion of pro-inflammatory TNF-α (Fig. 6B), IL-6 (Fig. 6C) and IL-8 (Fig. 6D), and further enhanced levels of the anti-inflammatory cytokine IL-10 (Fig. 6E). Furthermore, α2,8 NANA-NP were also shown to limit the activation of NFκB through preventing the degradation of IκB (Fig. S6). Comparable results were observed with primary human monocytes and, although the degree of pro-inflammatory cytokine inhibition was less pronounced in comparison to MDM, TNF-α was nevertheless significantly attenuated (Fig. 6G, 6H and 6I). To assess possible toxicity, we examined IL-1β secretions in human MDM. Analogous to PBS controls, α2,8 NANA-NP did not induce IL-1β production (Fig. S5).

We next investigated the feasibility of this treatment in attenuating inflammation in a human ex vivo lung perfusion (EVLP) model (Fig. S7) (32-34). Injury was induced through intrabronchial instillation of LPS and α2,8 NANA-NP or saline control treatment were added to the perfusate to model systemic administration in a randomized blinded manner. Pulmonary edema, the hallmark of ARDS, was measured via tissue wet/dry ratios (Fig. 6J), and BAL fluid IL-10 was also analysed (Fig. S6). Compared to controls, treatment with α2,8 NANA-NP induced a significant reduction in these wet/dry ratios.

Discussion:

Previously we have demonstrated that multivalent display of antibodies on the surface of nanoparticles can facilitate targeting to a given cell type and also elicits receptor clustering and activation, triggering downstream responses that are not achievable with free antibody (16, 35-38). In this current study, we devised an alternative strategy to induce specific Siglec activation and produce therapeutic effects. In lieu of antibodies, we employed a physiological ligand of mouse Siglec-E and its human equivalents (39). We demonstrated that α2,8-linked disialic acid elicited anti-inflammatory effects only when coated onto PLGA nanoparticles. We then showed that these nanoparticles produced therapeutically useful anti-inflammatory effects in a range of murine and human inflammatory models.

Boyd *et al* (11) showed that activated Siglec-E recruited SHP phosphatases in order to ameliorate LPS-induced signaling through reduction of IL-6 and TNF-α secretions. The downstream effects of this nanoparticle engagement in both murine and human model systems were in agreement with the previously reported findings. We showed that α2,8 NANA-NP can specifically target Siglec-E and reduce inflammatory cytokine production in models of systemic inflammation and localized lung injury. McMillan *et al* (10) reported that lung neutrophilia was exacerbated in a murine model of ARDS in a Siglec-E deficient background. Similarly, we found that nanoparticle-mediated activation of Siglec-E attenuated pulmonary neutrophil counts.

In response to reports verifying the expression of Siglec-E on other cell types such as neutrophils (10,39), we examined the cellular targets of α2,8 NANA-NP. Upon i.p. administration of fluorescent α2,8 NANA-NP macrophages appeared to be the primary target, expressing higher levels of Siglec-E compared to neutrophils. The functionality of the nanoparticles appeared to be neutrophil-independent as the ability of these nanoparticles to rescue animals from lethal inflammation was attenuated following macrophage depletion. Hypothetically, in contrast to macrophages, α2,8 NANA-NP may be unable to cross-link Siglec-E on neutrophils to the extent needed for sufficient activation. Recently, a newly described innate response activator B cell population was shown to play an important role in bacterial clearance and sepsis associated cytokine responses (40). Our data suggest that macrophage populations are the predominant targeted cell population by α2,8 NANA-NP and are largely responsible for our observed anti-inflammatory effectiveness, however, our experiments cannot completely exclude that our functionalized nanoparticles could directly or indirectly influence these newly described innate effector B cells.

Our previous studies hypothesized that Siglec-E, and potentially other human equivalents, were upregulated in a negative feedback manner to return cells to homeostasis. While LPS was able to potently upregulate the expression of Siglec-E in mouse macrophages, this was not significant in human MDM, confirming other reports (41). While investigating this dichotomy, we noted that LPS could enhance IL-10 production in both settings and this was further potentiated on co-treatment with α2,8 NANA-NP. Others have reported that LPS-induced IL-10 has an important role in attenuating pro-inflammatory responses and maintaining tolerance, and this thus highlights an important role for Siglecs in homeostatic and anti-inflammatory responses (42).

This alternative approach to targeting Siglec receptors extends the findings of Boyd *et al* (11). We report that IL-10 is fundamental for the downstream expression of Siglec-E after LPS stimulation. Moreover, we confirm our previous finding that this Siglec-E induction pathway is also MyD88 dependent. We propose

that this negative feedback pathway is exploited by α2,8 NANA-NP to block pro-inflammatory responses and enhance resolution (Fig. S7). In an inflammatory setting, α2,8 NANA-NP engages Siglec-E and potentiates inhibitory pathways, including recruitment of SHP-2 and NFκB p50 dimer translocation to the nucleus. Elevated production of IL-10 then leads to further Siglec-E expression, enhancing the available receptors for nanoparticle binding. Activation of Siglec-E by cross-linking nanoparticles potently induces further secretion of IL-10. Importantly, the restoration of normal immune cell function is possible owing to the biocompatible and biodegradable nature of this PLGA platform.

The consequences of Siglec-E activation observed here with our nanoparticle are consistent with an indirect approach to Siglec modulation using sialidase inhibitors to preserve Siglec-G signal transduction, inhibiting sepsis progression (43). Läubli *et al* (44) have recently described the inhibitory effects of Siglec-9 engagement on human neutrophils and macrophages with tumor expressed sialic acid. Other data show the strategies evolved by bacteria and viruses to evade immunosurveillance mechanisms (45, 46) and enhance dissemination and survival. Interestingly, a variety of sialic acid-bearing 'nanocarriers' have been described before. For instance, different sialic acid variants have been exploited to selectively deliver chemotherapeutics to B cells or to enhance nano-surface hydrophilicity, thus improving bioavailability (47-50). In another report, liposomes decorated with high affinity Siglec-7 ligands enabled efficient delivery of mycobacterial ligands to dendritic cells, resulting in a robust T cell immune response (51). Similarly, a liposomal formulation was designed to target macrophage-expressed sialoadhesin, which also elicited T cell activation (52).

In conclusion, we have developed a Siglec-targeting approach that is distinct from other reported strategies. Here we have shown that nanoparticle surface display of sialic acid promotes oligomerization and activation of Siglecs on macrophages. We have been able to exploit this effect to elicit therapeutically useful effects in murine models of systemic and pulmonary inflammation. Crucially, we have demonstrated the translational potential of α2,8 NANA-NP in human assays, including an EVLP model, which currently represents the most advanced pre-clinical model for lung-targeting therapeutics. Taken together our findings validate this nanotherapeutic approach, and confirm Siglecs as drugable anti-inflammatory targets.

Materials and Methods:

Mice: C57BL/6 specific pathogen free WT mice were purchased from Harlan Laboratories (UK) and used at 6-8 weeks. IL-$10^{-/-}$ (C57BL/6 Background) mice were a kind gift of the MGC Foundation (53). All experiments were sanctioned by the UK Home Office and approved by Queen's University Belfast Ethical

Review Committee or Irish Department of Health and Children and Trinity College Dublin Bioresources Ethical Review Board.

Cell preparation and culture: Peritoneal macrophages were collected through injection of sterile PBS into the peritoneal cavity of WT mice. Cells were lavaged and washed once with PBS prior to counting and adherence to culture plates for 2hr. Non-adherent cells were discarded, whilst adherent cells were collected by vigorous washing and characterized as macrophages by FACS as $CD11b^{+}F4/80^{+}$ cells. The murine macrophage RAW 264.7 cell line was obtained from the American Type Culture Collection and immortalised WT or $MyD88^{-/-}$ murine BMDM were a kind gift from Prof. Andrew Bowie (Trinity College Dublin). The above cells were cultured in DMEM supplemented with 10% low-endotoxin foetal calf serum, 1% penicillin/streptomycin and 1% L-glutamine (subsequently referred to as complete DMEM) (PAA) during stimulations at 37°C, 5% CO_2. Primary murine BMDM were prepared from C57BL/6 WT mice and cultured for one week in complete DMEM. Differentiation was driven by granulocyte macrophage-colony stimulating factor (GM-CSF) derived from L929 supernatant. Human monocytes were isolated from healthy donor buffy coats by centrifugation across a Ficoll-Paque gradient (GE Healthcare), followed by adherence purification. Cells were matured in RPMI supplemented with 10% low-endotoxin foetal calf serum, 1% penicillin/streptomycin and 1% L-glutamine. Differentiation of monocytes to macrophages was achieved through the addition of 10ng/mL GM-CSF (Peprotech) to the culture media for seven days.

Study design:

The hypothesis of this investigation was that PLGA nanoparticles coated with a sialic acid ligand would inhibit inflammatory responses of macrophages and monocytes by binding to their cognate Siglec receptor on the cell surface. Investigations were designed to evaluate the impact of sialic acid coated nanoparticles compared to uncoated nanoparticle and ligand controls. This hypothesis was tested in various human and murine models of inflammation and experimental replication is defined within the appropriate figure legends. In vivo studies were carried out on littermate animals to minimise variances between groups. The number of animals within each study arm is denoted within the appropriate figure legends. Ethical approval for the use of buffy coat residue from anonymized healthy blood donors for monocyte isolation was obtained from the Northern Ireland Blood Transfusion Service. Experiments were repeated from multiple donors to minimize bias. Human lungs for the EVLP studies were obtained and used with approval from the International Institute for the Advancement of Medicine (IIAM). Ethical approval for the use of lungs and human donor blood in the EVLP model was obtained from Queen's University Belfast School of Medicine, Dentistry and Biomedical Sciences School Research Ethics Committee. Both EVLP and CLP studies were conducted in a blinded manner.

Evaluation of the anti-inflammatory effects of α2,8 NANA-NP: Peritoneal macrophages were stimulated with 100ng/mL *Escherichia coli* R515 LPS (Invivogen) ± nanoparticles as specified in the appropriate figure legends. Murine BMDM were stimulated with 1ng/mL LPS overnight to upregulate Siglec-E. BMDM were washed twice in serum-free DMEM prior to resting for 2hr. BMDM were re-stimulated with 100ng/mL LPS ± nanoparticles.

Fluorescence Microscopy Imaging: RAW 264.7 cells were seeded on glass cover slips in six-well plates at $2.5x10^5$ cells per well and cultured overnight. Cells were stimulated for 3hr with 0.25μg/mL coumarin 6-loaded nanoparticles in serum-free DMEM. Cells were washed three times with ice-cold PBS, fixed in 4% paraformaldehyde for 1hr and washed a further three times as above. Cells were incubated for 30min in HEPES buffer (0.1M; pH 8) and washed again as above. For nuclear staining, cells were incubated with a 1:200 solution of TO-PRO-3 iodide (Invitrogen) and subsequently washed three times with ice-cold PBS. Cells were visualised by mounting coverslips onto microscope slides using Slow Fade Gold reagent (Invitrogen). Sample analyses were performed using confocal scanning laser microscopy (Leica Confocal TCS Sp2) with laser illumination at 488nm for green fluorescence, 543nm for red fluorescence and 633nm for far-red fluorescence.

Attenuation of Siglec-E activity: Blocking of Siglec-E dependent binding was achieved by 2hr pre-treatment of cells with 10μg/mL anti-Siglec-E (Antibodies-online) or IgG isotype (Fusion Antibodies), prior to stimulation with LPS, nanoparticles or controls. WT peritoneal macrophages were plated at $5x10^5$ cells/well in 24 well plates. Siglec-E gene silencing was accomplished by transfecting macrophages with genecellin nanoporters encapsulating 2μg of scrambled shRNA or Siglec-E specific shRNA (Origene)(11) for 48hr as per manufacturer's instructions. Following transfection, macrophages were stimulated for another 24hr with 100ng/mL LPS ± 125μg/mL nanoparticles.

Immunoblotting and evaluation of NFκB: Immunoprecipitation of Siglec-E (R&D Systems) and analyses of SHP-2 (Santa-Cruz) by western blot was performed as described previously (11) using lysates from LPS ± nanoparticle-treated C57BL/6 macrophages. γ Tubulin was probed as a loading control (Sigma Aldrich). Nuclear translocation of NFκB p50 and p65 subunits was assessed using the colorimetric NFκB p50/p65 EZ-TFA transcription factor assay (Millipore) according to the manufacturer's instructions.

Model of LPS-induced systemic inflammation: C57BL/6 WT or $IL10^{-/-}$ mice were treated with i.p. injections of 6mg/kg LPS ± nanoparticles or controls dispersed in PBS. Mice were monitored over 50hr as per UK Home Office guidelines. Mice were culled immediately at a humane end-point noted by loss of self-righting and insensitivity to touch. Serum was sampled from tail-vein bleeds at specified time-points and analyzed by ELISA. Serum was obtained by allowing blood to clot at room temperature for 30min prior to centrifugation at 14000*g* for 10min.

Model of LPS-induced acute lung inflammation: C57BL/6 WT mice were anaesthetized and suspended on an endotracheal intubation platform (Penn-Century). A LS-2-M laryngoscope (Penn-Century) was used to illuminate the trachea and a blunt 24G IV catheter (BD) was positioned between the vocal cords. A total volume of 50μL was instilled into the lungs via the catheter, containing 20μg LPS in PBS. At 2hr following LPS instillation, 2mg α2,8 NANA-NP or Nude-NP were injected i.p. Mice were then sacrificed 24hr post-LPS instillation. To facilitate collection of BAL fluid, a blunt 23G needle was placed within a small opening in the upper trachea and secured in position with Mersilk suture (Ethicon). The lungs were lavaged with a total volume of 700μL ice-cold PBS, which was instilled in 350μL aliquots via the tracheal cannula, followed by gentle aspiration. BAL fluid was centrifuged at 425*g* for 10min at 4^{o}C and the cell pellets were resuspended in 100μL ice-cold PBS. Total viable cell counts were conducted using a haemocytometer under trypan blue exclusion. Following collection of BAL fluid, lung lobes were homogenized in a TissueLyser LT (Qiagen) for 4min. Samples were centrifuged at 18000*g* for 15min at 4^{o}C and supernatant cytokine levels were quantified by ELISA.

Cytocentrifugation, cell staining and differential counts: Approximately 1 x 10^5 cells from each BAL fluid sample were cytocentrifuged onto coated cytoslides (Shandon Thermo Scientific) for 5min. Following fixation in methanol for 20min, the slides were dried at room temperature and then stained in May-Grünwald solution (VWR) for 8min. The cytospins were washed quickly in distilled water and submerged in Giemsa stain (VWR) for 8min. After two brief washes in PBS, the slides were dried at room temperature for 5min and a single drop of VectaMount™ AQ (Vector Laboratories) was added to each cytospin. Coverslips were then positioned and the slides were allowed to dry overnight. Representative images were captured at x40 magnification, using a DM5500B light microscope (Leica Microsystems) with Leica AL software (version 3.7). Differential counts were performed on a minimum of 400 white cells per cytospin.

Flow cytometric analyses: Human monocytes and macrophages were stimulated as described in Fig. 6 legend. Cells were stained with antibodies against Siglec-7-PE, Siglec-9-FITC or isotype controls (BD). In brief, cells were stained as per manufacturer's instructions for 30min on ice. Cells were washed with 3mL FACS Buffer, centrifuged at 500*g* for 5min at 4^{o}C and resuspended in 200μL FACS Buffer. Cells were analyzed using a FACSCantoII flow cytometer and FACSDiva (BD) and FLowJO software (Treestar). Representative plots shown.

Depletion of macrophages using clodronate liposomes: Clodronate liposomes or control PBS liposomes were purchased from clodronateliposomes.org. In brief, 300μL of liposomes were injected i.p. into appropriate mice groups 48hr and 24hr prior to LPS and nanoparticle treatment. Mice were monitored for survival as above and serum was collected 24hr after treatment for analysis of TNF-α by ELISA.

Depletion of F4/80+ macrophages was assessed by flow cytometry as described previously to determine percentage of depletion (representative data to ~90% depletion shown in Fig. S3).

Induction of CLP-mediated sepsis: Polymicrobial sepsis was induced in male C57BL/6 WT mice using the CLP method as described (25). Briefly, following anaesthesia, the caecum was ligated below the ileo-caecal valve following midline laparotomy. Perforation of the caecum resulted in translocation of bacteria into the peritoneum and subsequent peritonitis. A defined severity of sepsis among animals was ensured with the uniform positioning of the ligation. Post-operative fluid resuscitation was provided with 1mL of sterile sodium chloride (37^{o}C) administered subcutaneously. Groups of mice were given α2,8 NANA-NP or Nude-NP (2mg/mouse), equivalent free α2,8 NANA (30μg/mouse) or dexamethasone (0.1mg/mouse) i.p. 2hr post-surgery and every subsequent 24hr. Temperature transponders (Plexx B.V.) were implanted subcutaneously pre-surgery and temperature recorded electronically (DAS-6007, Bio Medic Data Systems) before and every 12hr post-surgery. Mice were scored every 12hr using the following criteria: score 0 – no symptoms; score 1 – piloerection, huddling; score 2 – piloerection, huddling, diarrhea; score 3 – lack of interest in surroundings, severe diarrhea; score 4 – decreased movement, listless appearance; and score 5 – loss of self-righting reflex. When mice reached score 5 they were humanely killed. Analgesia was provided throughout to all mice using buprenorphine.

Detection of secreted cytokines: DuoSet ELISA kits (R&D Systems) were used to detect concentrations of TNF-α, IL-6, IL-8, IL-10 and IL-1β within samples according to the manufacturer's instructions.

Real-time PCR: After appropriate stimulation, RNA was extracted using the RNeasy mini-kit (Qiagen). After conversion, 50ng first-strand cDNA was used in SYBR green reactions (Qiagen) using primers previously described (11). Siglec-E mRNA expression was analyzed and normalized to β-actin. Comparison of ΔΔCT values versus unstimulated levels was carried out using MxPRO QPCR Software (Version 4.10d) (Agilent technologies).

EVLP model: EVLP setup and operation was as previously described (34). Briefly, lung injury was induced by intrabronchial instillation of 6mg LPS. Saline or 5mg α2,8 NANA-NP were added simultaneously to the perfusate, thereby modeling systemic delivery. At 4hr post-injury, BAL was performed and tissue sections were excised for determination of wet/dry ratios to evaluate accumulation of alveolar fluid, as a marker of global lung injury. Tissue sections were weighed immediately to obtain the wet weight, then dried in an oven at 56^{o}C for 48hr and weighed again to determine the dry weight. Wet/dry ratios were calculated by dividing the wet weight by the dry weight.

Statistical analysis: Student t-test was used to determine significance of parametric data between two groups. Mann-Whitney U test was used to determine significance of non-parametric data between two groups. One-way ANOVA and Tukey post-hoc test was used to determine significance of parametric data between multiple groups. Two-way ANOVA and Bonferroni post-hoc test was used to determine

significance of parametric data between WT and IL-$10^{-/-}$ mice strains. Survival significance was assessed with Kaplan-Meier plot and Log Rank Chi square test. Statistical significance was denoted by asterisks in the appropriate figures (defined as: *$p<0.05$; **$p<0.01$; ***$p<0.001$), in comparison to LPS only control unless indicated otherwise. Error bars represent ± 1 standard error of the mean (± SEM).

Acknowledgements: We thank Prof. David Jones (Queen's University Belfast) for his assistance with statistical analyses and Lorraine Hanna, Stephen Lloyd and Mary Hanna (Queen's University Belfast) for aid with in vivo experiments.

Funding: This work was funded in part through an MRC DPFS project grant MR-J014680, awarded to CJS, AK, DFMcA, CMO'K and PGF.

Author contributions: SS, MG and FF conducted all experiments and drafted the manuscript. EH and SPS conducted CLP experiments. UH and MF conducted EVLP experiments. JB performed experiments relating to IL-10 dependent responses. BKB formulated nanoparticle preparations for animal studies. PS and ET characterized nanoparticle structure. DMS and DS helped design and undertake in vitro and in vivo experiments and aided manuscript preparation. CMO'K and DFMcA aided in experimental design for the human in vitro and ex vivo experiments, secured ethical approval for the use of human lungs, blood and buffy coats and aided in data interpretation and manuscript preparation. DF provided IL-$10^{-/-}$ animals and aided in experimental design. SMA characterized nanoparticle anti-inflammatory responses in vitro. JAJ, PGF, JFB, AK aided in experimental design and manuscript preparation. CJS conceptualized the project, aided experimental design and manuscript preparation.

Competing interests: CJS, JAJ, SS, FF and DFMcA hold patent US8962032. No other conflicts of interest to report.

Data and materials availability: Data and material are available upon reasonable request.

List of Supplementary materials:

Fig. S7. Schematic of EVLP model and proposed mechanism of action of α2,8 NANA-NP

References

1) M. Singer, Biomarkers in sepsis. *Curr. Opin. Pulm. Med*. **19**, 305-309 (2013).

2) P. E. Marik, Early management of severe sepsis: concepts and controversies. *Chest* **145**, 1407-1418 (2014).

3) C. Brun-Buisson, C. Minelli, G. Bertolini, L. Brazzi, J. Pimentel, K. Lewandowski, J. Bion, J. A. Romand, J. Villar, A. Thorsteinsson, P. Damas, A. Armaganidis, F. Lemaire, Epidemiology and outcome of acute lung injury in European intensive care units. Results from the ALIVE study. *Intensive Care Med*. **30**, 51-61 (2004).

4) D. F. McAuley, J. G. Laffey, C. M. O'Kane, G. D. Perkins, B. Mullan, T. J. Trinder, P. Johnston, P. A. Hopkins, A. J. Johnston, C. McDowell, C. McNally; HARP-2 Investigators; Irish Critical Care Trials Group, Simvastatin in the acute respiratory distress syndrome. *N. Engl. J. Med*. **371**, 1695-1703 (2014).

5) T. Kawai, S. Akira, TLR signaling. *Semin. Immunol.* **19**, 24-32 (2007).

6) M. Ando, W. Tu, K. Nishijima, S. Iijima, Siglec-9 enhances IL-10 production in macrophages via tyrosine-based motifs. *Biochem. Biophys. Res. Commun.* **369**, 878-883 (2008).

7) D. Y. Mason, H. Stein, J. Gerdes, K. A. Pulford, E. Ralfkiaer, B. Falini, W. N. Erber, K. Micklem, K. C. Gatter, Value of monoclonal anti-CD22 (p135) antibodies for the detection of normal and neoplastic B lymphoid cells. *Blood* **69**, 836-840 (1987).

8) P. R. Crocker, Siglecs in innate immunity. *Curr. Opin. Pharmacol.* **5**, 431-437 (2005).

9) M. K. O'Reilly, J. C. Paulson, Siglecs as targets for therapy in immune-cell-mediated disease. *Trends Pharmacol. Sci.* **30**, 240-248 (2009).

10) S. J. McMillan, R. S. Sharma, E. J. McKenzie, H. E. Richards, J. Zhang, A. Prescott, P. R. Crocker, Siglec-E is a negative regulator of acute pulmonary neutrophil inflammation and suppresses CD11b β2-integrin-dependent signaling. *Blood* **121**, 2084-2094 (2013).

11) C. R. Boyd, S. J. Orr, S. Spence, J. F. Burrows, J. Elliott, H. P. Carroll, K. Brennan, J. Ní Gabhann, W. A. Coulter, C. Jones, P. R. Crocker, J. A. Johnston, C. A. Jefferies, Siglec-E is up-regulated and phosphorylated following lipopolysaccharide stimulation in order to limit TLR-driven cytokine production. *J. Immunol.* **183**, 7703-7709 (2009).

12) S. Mizrahi, B. F. Gibbs, L. Karra, M. Ben-Zimra, F. Levi-Schaffer, Siglec-7 is an inhibitory receptor on human mast cells and basophils. *J. Allergy Clin. Immunol*. **134**, 230-233 (2014).

13) K. Miyazaki, K. Sakuma, Y. I. Kawamura, M. Izawa, K. Ohmori, M. Mitsuki, T. Yamaji, Y. Hashimoto, A. Suzuki, Y. Saito, T. Dohi, R. Kannagi, Colonic epithelial cells express specific ligands for mucosal macrophage immunosuppressive receptors siglec-7 and -9. *J. Immunol*. **188**, 4690-4700 (2012).

14) L. Nitschke, H. Floyd, P. R. Crocker, New functions for the sialic acid-binding adhesion molecule CD22, a member of the growing family of Siglecs. *Scand. J. Immunol.* **53**, 227-234 (2001).

15) E. C. Brinkman-Van der Linden, A. Varki, New aspects of siglec binding specificities, including the significance of fucosylation and of the sialyl-Tn epitope. *J. Biol. Chem.* **275**, 8625-8632 (2000).

16) C. J. Scott, W. M. Marouf, D. J. Quinn, R. J. Buick, S. J. Orr, R. F. Donnelly, P. A. McCarron, Immunocolloidal targeting of the endocytotic siglec-7 receptor using peripheral attachment of siglec-7 antibodies to poly(lactide-co-glycolide) nanoparticles. *Pharm. Res.* **25**, 135-146 (2008).

17) C. Jandus, H. U. Simon, S. von Gunten, Targeting siglecs – a novel pharmacological strategy for immuno- and glycotherapy. *Biochem. Pharmacol*. **82**, 323-332 (2011).

18) C. S. Fuchs, M. Fakih, L. Schwartzberg, A. L. Cohn, L. Yee, L. Dreisbach, M. F. Kozloff, Y. J. Hei, F. Galimi, Y. Pan, V. Haddad, C. P. Hsu, A. Sabin, L. Saltz, TRAIL receptor agonist conatumumab with modified FOLFOX6 plus bevacizumab for first-line treatment of metastatic colorectal cancer: A randomized phase 1b/2 trial. *Cancer* **119**, 4290-4298 (2013).

19) P. A. McCarron, R. F. Donnelly, W. M. Marouf, Celecoxib-loaded poly(D,L-lactide-co-glycolide) nanoparticles prepared using a novel and controllable combination of diffusion and emulsification steps as part of the salting-out procedure. *J. Microencapsul.* **23**, 480-498 (2006).

20) B. Sulzer, R. J. De Boer, A. S. Perelson, Cross-linking reconsidered: binding and cross-linking fields and the cellular response. *Biophys. J*. **70**, 1154-1168 (1996).

21) B. D. Harms, J. D. Kearns, S. Iadevaia, A. A. Lugovskoy, Understanding the role of cross-arm binding efficiency in the activity of monoclonal and multispecific therapeutic antibodies. *Methods* **65**, 95-104 (2014).

22) J. E. Juskewitch, J. L. Platt, B. E. Knudsen, K. L. Knutson, G. J. Brunn, J. P. Grande, Disparate roles of marrow- and parenchymal cell-derived TLR4 signaling in murine LPS-induced systemic inflammation. *Sci. Rep*. **2**, 918 (2012).

23) J. D. Veltman, M. E. Lambers, M. van Nimwegen, R. W. Hendriks, H. C. Hoogsteden, J. P. Hegmans, J. G. Aerts, Zoledronic acid impairs myeloid differentiation to tumour-associated macrophages in mesothelioma. *Br. J. Cancer* **103**, 629-641 (2010).

24) D. Rittirsch, M. S. Huber-Lang, M. A. Flierl, P. A. Ward, Immunodesign of experimental sepsis by cecal ligation and puncture. *Nat. Protoc.* **4**, 31-36 (2009).

25) E. Hams, S. P. Saunders, E. P. Cummins, A. O'Connor, M. T. Tambuwala, W. M. Gallagher, A. Byrne, A. Campos-Torres, P. M. Moynagh, C. Jobin, C. T. Taylor, P. G. Fallon, The hydroxylase inhibitor dimethyloxallyl glycine attenuates endotoxic shock via alternative activation of macrophages and IL-10 production by B1 cells. *Shock* **36**, 295-302 (2011).

26) G. Matute-Bello, C. W. Frevert, T. R. Martin, Animal models of acute lung injury. *Am. J. Physiol. Lung Cell. Mol. Physiol*. **295**, L379-399 (2008).

27) J. A. Bastarache, T. S. Blackwell, Development of animal models for the acute respiratory distress syndrome. *Dis. Model. Mech*. **2**, 218-223 (2009).

28) L. K. Reiss, U. Uhlig, S. Uhlig, Models and mechanisms of acute lung injury caused by direct insults. *Eur. J. Cell Biol*. **91**, 590-601 (2012).

29) N. Matsuda, Y. Hattori, S. Jesmin, S. Gando, Nuclear factor-kappaB decoy oligodeoxynucleotides prevent acute lung injury in mice with cecal ligation and puncture-induced sepsis. *Mol. Pharmacol*. **67**, 1018-1025 (2005).

30) L. Zhang, S. Jin, C. Wang, R. Jiang, J. Wan, Histone deacetylase inhibitors attenuate acute lung injury during cecal ligation and puncture-induced polymicrobial sepsis. *World J. Surg*. **34**, 1676-1683 (2010).

31) H. Björkbacka, K. A. Fitzgerald, F. Huet, X. Li, J. A. Gregory, M. A. Lee, C. M. Ordija, N. E. Dowley, D. T. Golenbock, M. W. Freeman, The induction of macrophage gene expression by LPS predominantly utilizes Myd88-independent signaling cascades. *Physiol Genomics* **19**, 319-330 (2004).

32) J. W. Lee, X. Fang, N. Gupta, V. Serikov, M. A. Matthay, Allogeneic human mesenchymal stem cells for treatment of E. coli endotoxin-induced acute lung injury in the ex vivo perfused human lung. *Proc. Natl. Acad. Sci. U. S. A*. **106**, 16357-16362 (2009).

33) J. W. Lee, A. Krasnodembskaya, D. H. McKenna, Y. Song, J. Abbott, M. A. Matthay, Therapeutic effects of human mesenchymal stem cells in ex vivo human lungs injured with live bacteria. *Am. J. Respir. Crit. Care Med*. **187**, 751-760 (2013).

34) D. F. McAuley, G. F. Curley, U. I. Hamid, J. G. Laffey, J. Abbott, D. H. McKenna, X. Fang, M. A. Matthay, J. W. Lee, Clinical grade allogeneic human mesenchymal stem cells restore alveolar fluid clearance in human lungs rejected for transplantation. *Am. J. Physiol. Lung Cell. Mol. Physiol*. **306**, L809-815 (2014).

35) F. Fay, K. M. McLaughlin, D. M. Small, D. A. Fennell, P. G. Johnston, D. B. Longley, C. J. Scott, Conatumumab (AMG 655) coated nanoparticles for targeted pro-apoptotic drug delivery. *Biomaterials* **32**, 8645-8653 (2011).

36) P. A. McCarron, W. M. Marouf, D. J. Quinn, F. Fay, R. E. Burden, S. A. Olwill, C. J. Scott, Antibody targeting of camptothecin-loaded PLGA nanoparticles to tumor cells. *Bioconjug. Chem.* **19**, 1561-1569 (2008).

37) S. M. Abdelghany, D. Schmid, J. Deacon, J. Jaworski, F. Fay, K. M. McLaughlin, J. A. Gormley, J. F. Burrows, D. B. Longley, R. F. Donnelly, C. J. Scott, Enhanced antitumor activity of the

photosensitizer meso-Tetra(N-methyl-4-pyridyl) porphine tetra tosylate through encapsulation in antibody-targeted chitosan/alginate nanoparticles. *Biomacromolecules* **14**, 302-310 (2013).

38) D. Schmid, F. Fay, D. M. Small, J. Jaworski, J. S. Riley, D. Tegazzini, C. Fenning, D. S. Jones, P. G. Johnston, D. B. Longley, C. J. Scott, Efficient drug delivery and induction of apoptosis in colorectal tumors using a death receptor 5-targeted nanomedicine. *Mol. Ther*. **22**, 2083-2092 (2014).

39) J. Q. Zhang, B. Biedermann, L. Nitschke, P. R. Crocker, The murine inhibitory receptor mSiglec-E is expressed broadly on cells of the innate immune system whereas mSiglec-F is restricted to eosinophils. *Eur. J. Immunol*. **34**, 1175-1184 (2004).

40) G. F. Weber, B. G. Chousterman, S. He, A. M. Fenn, M. Nairz, A. Anzai, T. Brenner, F. Uhle, Y. Iwamoto, C. S. Robbins, L. Noiret, S. L. Maier, T. Zönnchen, N. N. Rahbari, S. Schölch, A. Klotzsche-von Ameln, T. Chavakis, J. Weitz, S. Hofer, M. A. Weigand, M. Nahrendorf, R. Weissleder, F. K. Swirski, Interleukin-3 amplifies acute inflammation and is a potential therapeutic target in sepsis. *Science* **347**, 1260-1265 (2015).

41) K. Lock, J. Zhang, J. Lu, S. H. Lee, P. R. Crocker, Expression of CD33-related siglecs on human mononuclear phagocytes, monocyte-derived dendritic cells and plasmacytoid dendritic cells. *Immunobiology* **209**, 199-207 (2004).

42) A. Mantovani, F. Marchesi, IL-10 and macrophages orchestrate gut homeostasis. *Immunity* **40**, 637-639 (2014).

43) G. Y. Chen, X. Chen, S. King, K. A. Cavassani, J. Cheng, X. Zheng, H. Cao, H. Yu, J. Qu, D. Fang, W. Wu, X. F. Bai, J. Q. Liu, S. A. Woodiga, C. Chen, L. Sun, C. M. Hogaboam, S. L. Kunkel, P. Zheng, Y. Liu, Amelioration of sepsis by inhibiting sialidase-mediated disruption of the CD24-Siglec G interaction. *Nat. Biotechnol.* **29**, 428-435 (2011).

44) H. Läubli, O. M. Pearce, F. Schwarz, S. S. Siddiqui, L. Deng, M. A. Stanczak, L. Deng, A. Verhagen, P. Secrest, C. Lusk, A. G. Schwartz, N. M. Varki, J. D. Bui, A. Varki, Engagement of myelomonocytic Siglecs by tumor-associated ligands modulates the innate immune response to cancer. *Proc. Natl. Acad. Sci. U. S. A*. **111**, 14211-14216 (2014).

45) A. F. Carlin, S. Uchiyama, Y. C. Chang, A. L. Lewis, V. Nizet, A. Varki, Molecular mimicry of host sialylated glycans allows a bacterial pathogen to engage neutrophil Siglec-9 and dampen the innate immune response. *Blood* **113**, 3333-3336 (2009).

46) B. Khatua, S. Roy, C. Mandal, Sialic acids siglec interaction: a unique strategy to circumvent innate immune response by pathogens. *Indian J. Med. Res*. **138**, 648-662 (2013).

47) W. C. Chen, G. C. Completo, D. S. Sigal, P. R. Crocker, A. Saven, J. C. Paulson, In vivo targeting of B-cell lymphoma with glycan ligands of CD22. *Blood* **115**, 4778-4786 (2010).

48) W. C. Chen, D. S. Sigal, A. Saven, J. C. Paulson, Targeting B lymphoma with nanoparticles bearing glycan ligands of CD22. *Leuk. Lymphoma* **53**, 208-210 (2012).

49) L. Bondioli, L. Costantino, A. Ballestrazzi, D. Lucchesi, D. Boraschi, F. Pellati, S. Benvenuti, G. Tosi, M. A. Vandelli, PLGA nanoparticles surface decorated with the sialic acid, N-acetylneuraminic acid. *Biomaterials* **31**, 3395-3403 (2010).

50) G. Tosi, A. V. Vergoni, B. Ruozi, L. Bondioli, L. Badiali, F. Rivasi, L. Costantino, F. Forni, M. A. Vandelli, Sialic acid and glycopeptides conjugated PLGA nanoparticles for central nervous system targeting: In vivo pharmacological evidence and biodistribution. *J. Control. Release* **145**, 49-57 (2010).

51) N. Kawasaki, C. D. Rillahan, T. Y. Cheng, I. Van Rhijn, M. S. Macauley, D. B. Moody, J. C. Paulson, Targeted delivery of mycobacterial antigens to human dendritic cells via Siglec-7 induces robust T cell activation. *J. Immunol*. **193**, 1560-1566 (2014).

52) W. C. Chen, N. Kawasaki, C. M. Nycholat, S. Han, J. Pilotte, P. R. Crocker, J. C. Paulson, Antigen delivery to macrophages using liposomal nanoparticles targeting sialoadhesin/CD169. *PLoS One* **7**, e39039 (2012).

53) R. Kühn, J. Löhler, D. Rennick, K. Rajewsky, W. Müller, Interleukin-10-deficient mice develop chronic enterocolitis. *Cell* **75**, 263-274 (1993).

Figure Legends

Fig. 1. α2,8 NANA-NP targets Siglec-E on macrophages to limit LPS-driven pro-inflammatory cytokine production in vitro. **(A and B)** C57BL/6 peritoneal macrophages were stimulated with 100ng/mL LPS ± 125μg/mL α2,8 NANA-NP or appropriate controls for 12hr. Controls included α2,8 NANA alone (α2,8 NANA; equivalent amount as attached to α2,8 NANA-NP surface), non-functionalized nanoparticles (Nude-NP; 125μg/mL) and nanoparticles displaying a control polysaccharide (Glucosamine NP; 125μg/mL). Supernatants were assayed for TNF-α (A) and IL-6 (B) by ELISA. Statistical significance was assessed by one way ANOVA with post-hoc Tukey test (***$p<0.001$, in comparison to LPS only). Data expressed as mean + SEM (n = 3 independent experiments in triplicate). **(C)** C57BL/6 peritoneal macrophages were stimulated with 100ng/mL LPS or media alone for 24hr. mRNA was extracted, converted to cDNA and analyzed by real-time PCR for *Siglece* gene expression. Data are expressed as fold change relative to untreated samples and normalized to *β–actin* gene expression. Data expressed as mean + SEM (n = 3 independent experiments in triplicate). **(D and E)** C57BL/6 peritoneal macrophages (D) or BMDM (E) were treated with the stated dose of LPS for 0, 12 and 24hr. Macrophages were lysed in RIPA prior to analysis of Siglec-E and γ Tubulin protein by Western blot (representative images of n = 4 independent experiments). **(F)** C57BL/6 BMDM were stimulated with 1ng/mL LPS overnight to upregulate Siglec-E expression. Following 2hr pre-blocking with 10μg/mL anti-Siglec-E antibody, BMDM were stimulated with 100ng/mL LPS ± 125μg/mL α2,8 NANA-NP or Nude-NP for 12hr. Supernatants were assayed for TNF-α by ELISA. Statistical significance was assessed by one way ANOVA with post-hoc Tukey test (***$p<0.001$, in comparison to LPS only). Data expressed as mean + SEM (n = 3 independent experiments in triplicate). **(G)** C57BL/6 peritoneal macrophages were incubated with Siglec-E specific short hairpin RNA (shRNA) or scrambled shRNA encapsulated genecellin nanoporters for 48hr. Macrophages were then stimulated with 100ng/mL LPS ± 125μg/mL α2,8 NANA-NP or Nude-NP for 24hr. Supernatants were assayed for TNF-α by ELISA. Statistical significance was assessed by one way ANOVA with post-hoc Tukey test (**$p<0.01$, in comparison to scrambled shRNA LPS only). Data expressed as mean + SEM (n = 3 independent experiments in triplicate). **(H)** Confocal fluorescence microscopy images of unstimulated RAW 264.7 cells (left panels) or RAW 264.7 cells incubated with 125μg/mL coumarin 6-loaded Nude-NP (green; middle panels) or coumarin 6-loaded α2,8 NANA-NP (green; right panels) for 3hr. Nuclei were distinguished by To-Pro-3 staining (blue) (representative images of n = 3 independent experiments). **(I)** Confocal fluorescence microscopy images of RAW 264.7 cells incubated with 125μg/mL coumarin 6-loaded α2,8 NANA-NP (green; left panels). Alternatively RAW 264.7 cells were pre-incubated with control (IgG1; middle panels) or free anti-Siglec-E (anti-Siglec-E; right panels) antibodies for 3hr and then incubated with coumarin 6-loaded α2,8 NANA-

NP (green). Nuclei were distinguished by To-Pro-3 staining (blue) (representative images of n = 3 independent experiments).

Fig. 2. α2,8 NANA-NP attenuates systemic inflammation in murine models**. (A)** C57BL/6 mice (n = 8 per group) were treated with i.p. injections of 6mg/kg LPS in conjunction with 2mg α2,8 NANA-NP or Nude-NP, or treated with 2mg α2,8 NANA-NP only. Survival was monitored for 50hr. Statistical significance was assessed by Kaplan-Meier Log Rank Chi square test (***$p<0.001$). (**B and C**) At 24hr post-injection, blood samples were taken from mice by tail vein puncture and serum was assayed for TNF-α (B) and IL-10 (C) by ELISA. Statistical significance was assessed by one way ANOVA with post-hoc Tukey test (***$p<0.001$). Data expressed as mean + SEM. **(D)** C57BL/6 mice (n = 4 per group) were treated with i.p. injections of 6mg/kg LPS (or PBS for α2,8 NANA-NP only control). After 2hr, 2mg α2,8 NANA-NP or Nude-NP were injected i.p. Survival was monitored for 50hr. Statistical significance was assessed by Kaplan-Meier Log Rank Chi square test (**$p<0.01$). **(E and F)** At 24hr post-LPS injection, blood samples were taken from mice by tail vein puncture and serum was assayed for TNF-α (E) and IL-10 (F) by ELISA. Data expressed as mean + SEM. **(G)** C57BL/6 mice (n = 8 per group) were treated with i.p. injections of clodronate liposomes or PBS control liposomes at -48hr and -24hr. All groups were then treated with i.p. injections of 6mg/kg LPS in conjunction with 1mg α2,8 NANA-NP or Nude-NP. Survival was monitored for 50hr. Statistical significance was assessed by Kaplan-Meier Log Rank Chi square test (***$p<0.001$, between control liposome + α2,8 NANA-NP and control liposome + Nude-NP groups). **(H)** CLP was performed on C57BL/6 mice (n = 8-10 per group), followed by i.p. injection of 2mg α2,8 NANA-NP, 2mg Nude-NP, equivalent dosage of α2,8 NANA alone or 100μg dexamethasone 2hr after surgery and every 24hr subsequently. Survival was monitored for 9 days. Statistical significance was assessed by Kaplan-Meier Log Rank Chi square test (***$p<0.001$, between α2,8 NANA-NP and Nude-NP groups). **(I)** Clinical scoring post-CLP used the following criteria: score 0, no symptoms; score 1, piloerection, huddling; score 2, piloerection, huddling, diarrhea; score 3, lack of interest in surroundings, severe diarrhea; score 4, decreased movement, listless appearance; score 5, loss of self-righting reflex. Data expressed as mean ± SEM. **(J)** Body temperature post-CLP. Data expressed as mean ± SEM.

Fig. 3. α2,8 NANA-NP attenuates pulmonary inflammation in murine models. **(A and B)** C57BL/6 mice (n = 7-8 per group) were treated with 20μg LPS i.t. After 2hr, 2mg α2,8 NANA-NP or Nude-NP were injected i.p. Mice were sacrificed at 24hr post-LPS instillation, BAL fluid was collected and the lungs were then excised for further analyses. Neutrophil (A) and macrophage (B) counts in BAL fluid, as quantified from cytospin images. Statistical significance was assessed by Mann-Whitney U test (**$p<0.01$). Data expressed as mean + SEM. **(C)** Lung homogenate supernatants were assayed for IL-10 by ELISA. Statistical significance was assessed by Mann-Whitney U test (*$p<0.05$). Data expressed as mean + SEM. **(D)** CLP was performed on C57BL/6 mice (n = 12-13 per group at outset of experiment), followed by i.t. instillation of 20μg α2,8 NANA-NP or Nude-NP 6-8hr after surgery. Clinical scoring post-CLP used the following criteria: score 0, no symptoms; score 1, piloerection, huddling; score 2, piloerection, huddling, diarrhea; score 3, lack of interest in surroundings, severe diarrhea; score 4, decreased movement, listless appearance; score 5, loss of self-righting reflex. Statistical significance was assessed by Student's t-test (*$p<0.05$). Data expressed as mean ± SEM. **(E)** Survival was monitored for 96hr. **(F and G)** CLP was performed on C57BL/6 mice (n = 7-11 per group), followed by treatment as described in (D). Mice were sacrificed at 30hr post-treatment and BAL fluid was collected. Total cell (F) and neutrophil (G) counts in BAL fluid. Statistical significance was assessed by Student's t-test (*$p<0.05$). Data expressed as mean + SEM.

Fig. 4. α2,8 NANA-NP induces SHP-2 recruitment to Siglec-E to promote downstream anti-inflammatory responses. **(A)** C57BL/6 peritoneal macrophages were pre-treated with 125μg/mL α2,8 NANA-NP or Nude-NP for 24hr prior to stimulation with 100ng/mL LPS for 0, 12 or 24hr. Macrophages were lysed in RIPA and immunoprecipitated (IP) using anti-Siglec-E antibody. IP was blotted for SHP-2, whilst whole cell lysate was blotted for Siglec-E and SHP-2 protein expression (representative image of n = 3 independent experiments). **(B)** C57BL/6 peritoneal macrophages were treated with 125μg/mL α2,8 NANA-NP or Nude-NP in conjunction with 100ng/mL LPS. Nuclear localization of p50 was determined using the p50/p65 EZ-TFA colorimetric assay. Data presented as fold ratio of p50/p65 compared to control untreated cells. Statistical significance was assessed by one way ANOVA with post-hoc Tukey test (**$p<0.01$). Data expressed as mean + SEM (n = 3 independent experiments in duplicate). **(C)** Immortalised wild-type (WT) or MyD88-deficient ($MyD88^{-/-}$) BMDM were stimulated with 100ng/mL LPS ± 125μg/mL α2,8 NANA-NP for 24hr. Supernatants were assayed for IL-10 by ELISA. Statistical significance was assessed by two way ANOVA with post hoc Bonferroni test (*$p<0.05$). Data expressed as mean + SEM (n = 3 independent experiments in duplicate). **(D)** Immortalised WT or $MyD88^{-/-}$ BMDM were stimulated with 100ng/mL LPS or media alone for 24hr. Supernatants were assayed for IL-10 by

ELISA. Statistical significance was assessed by two way ANOVA with post hoc Bonferroni test (***$p<0.001$). Data expressed as mean + SEM (n = 3 independent experiments in duplicate).

Fig. 5. Siglec-E is induced by IL-10 and the anti-inflammatory effects of α2,8 NANA-NP are IL-10 dependent. **(A)** C57BL/6 peritoneal macrophages were stimulated with 100ng/mL LPS or 10ng/mL IL-10 for 24hr. mRNA was extracted, converted to cDNA and analyzed by real-time PCR for *Siglece* gene expression. Data are expressed as fold change relative to untreated samples and normalized to *β–actin* gene expression. Data expressed as mean + SEM (n = 3 independent experiments in triplicate). **(B)** C57BL/6 peritoneal macrophages were stimulated as in (A). Macrophages were lysed in RIPA prior to analysis of Siglec-E and γ Tubulin protein expression by Western blot (representative image of n = 3 independent experiments). **(C)** C57BL/6 peritoneal macrophages were pre-treated with 10 μg/mL IL-10 receptor blocking antibody or IgG1 isotype control overnight. Macrophages were then stimulated with 100 ng/mL LPS or 10 ng/mL IL-10 for 24hr. Macrophages were lysed in RIPA prior to analysis of Siglec-E and γ Tubulin protein expression by Western blot (representative image of n = 3 independent experiments). **(D)** C57BL/6 WT or IL-$10^{-/-}$ mice (n = 8 per group) were treated with i.p. injections of 6mg/kg LPS in conjunction with 1mg α2,8 NANA-NP or Nude-NP. Survival was monitored for 50 hr. Statistical significance was assessed by Kaplan-Meier Log Rank Chi square test (**$p<0.01$ between WT + α2,8 NANA-NP and WT + Nude-NP groups). **(E)** At 12hr post-injection, blood samples were taken from mice by tail vein puncture and serum was assayed for TNF-α by ELISA. Statistical significance was assessed by two way ANOVA with post hoc Bonferroni test (***$p<0.001$ between WT + α2,8 NANA-NP and WT + Nude-NP groups). Data expressed as mean + SEM.

Fig. 6. α2,8 NANA-NP promotes anti-inflammatory effects in human cell assays**. (A)** Primary human MDM (n = 4 donors) were stimulated with 500ng/mL LPS for 18hr. MDM were stained with Siglec-7-PE and Siglec-9-FITC or appropriate isotype control antibodies and analyzed by flow cytometry. Representative plots shown. **(B, C and D)** Primary human MDM (n = 6-13 donors) were pre-treated with 10ng/mL LPS for 1hr prior to addition of 25μg/mL α2,8 NANA-NP or Nude-NP for a further 12hr. Supernatants were assayed for TNF-α (B), IL-6 (C) and IL-8 (D) by ELISA. Data presented as % change in cytokine levels relative to MDM stimulated with LPS only. Statistical significance was assessed by Mann-Whitney U test (*$p<0.05$, ***$p<0.001$). Data expressed as mean ± SEM. **(E)** Primary human MDM (n = 3 donors) were stimulated with 10ng/mL LPS ± 50μg/mL α2,8 NANA-NP. Supernatants were assayed for IL-10 by ELISA. Data expressed as mean + SEM. **(F)** Primary human monocytes (n = 2 donors) were stimulated with 10ng/mL LPS for 24hr. Monocytes were stained with Siglec-7-PE and Siglec-9-FITC or appropriate isotype control antibodies and analyzed by flow cytometry. Representative

plots shown. **(G, H and I)** Primary human monocytes (n = 7 donors) were stimulated with 10ng/mL LPS ± 50μg/mL α2,8 NANA-NP or Nude-NP for 18hr. Supernatants were assayed for TNF-α (G), IL-6 (H) and IL-8 (I) by ELISA. Data presented as % change in cytokine levels relative to monocytes stimulated with LPS only. Statistical significance was assessed by Mann-Whitney U test (*$p<0.05$). Data expressed as mean ± SEM. **(J)** Human lungs (n = 3 per group) were injured ex vivo by intrabronchial instillation of 6mg LPS. Lungs were treated simultaneously with saline or 5mg α2,8 NANA-NP, which were introduced into the perfusate in order to model systemic administration. At 4hr post-treatment, lung tissue sections were excised for assessment of the wet/dry ratio (*$p<0.05$). Data expressed as mean ± SEM.

Fig. 1. α2,8 NANA-NP targets Siglec-E on macrophages to limit LPS-driven pro-inflammatory cytokine production in vitro

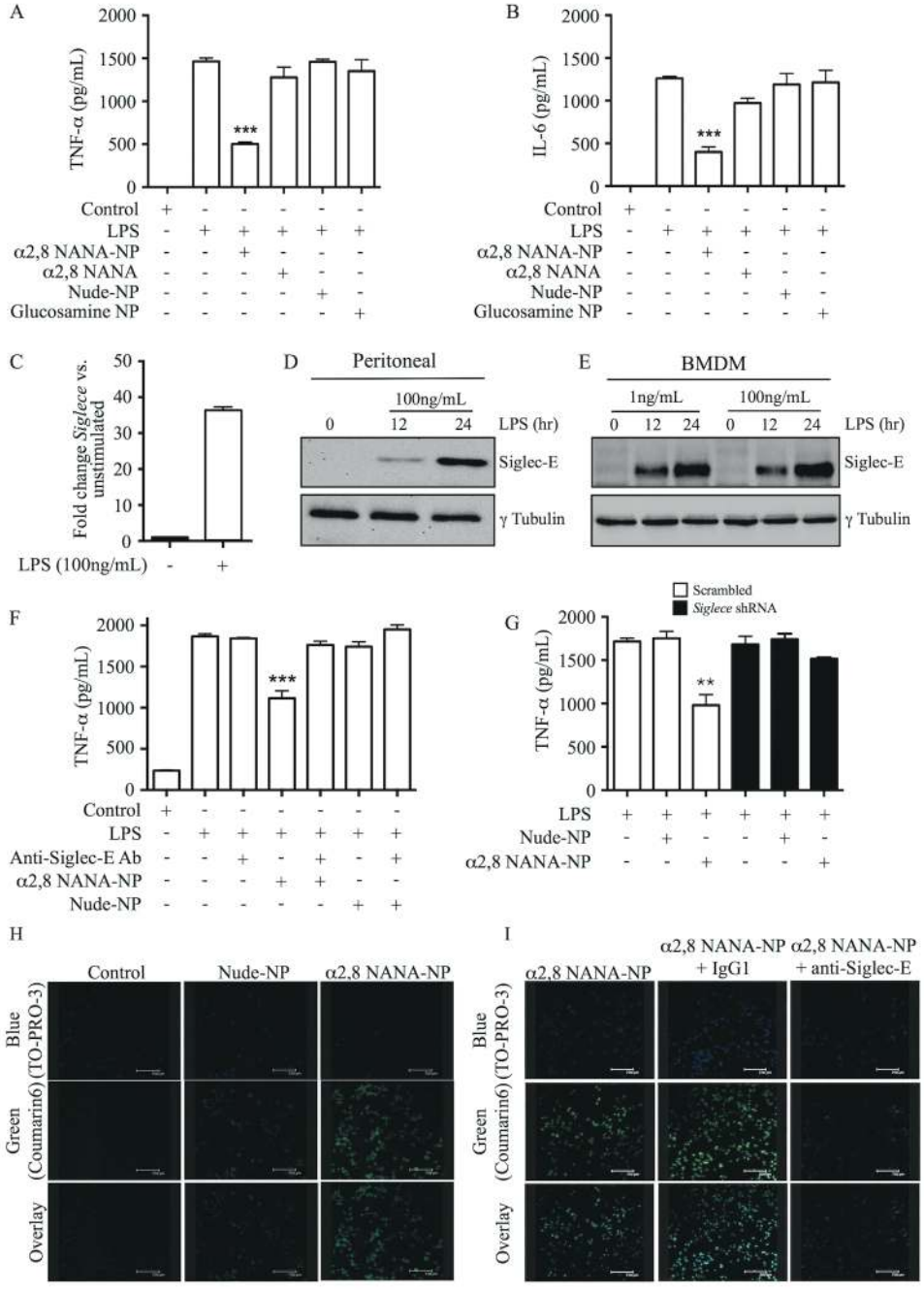

Fig. 2. α2,8 NANA-NP attenuates systemic inflammation in murine models

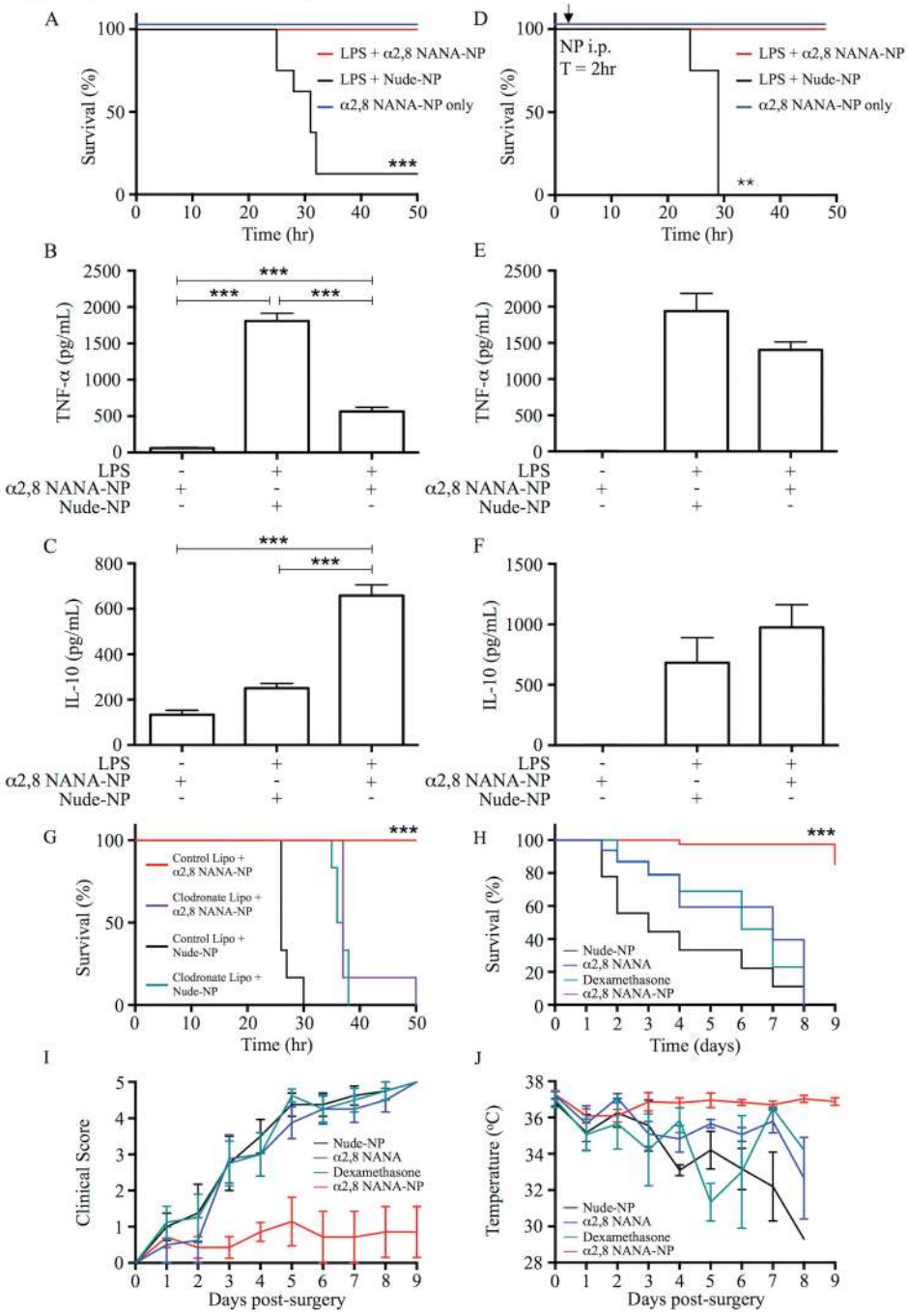

Fig. 3. α2,8 NANA-NP attenuates pulmonary inflammation in murine models

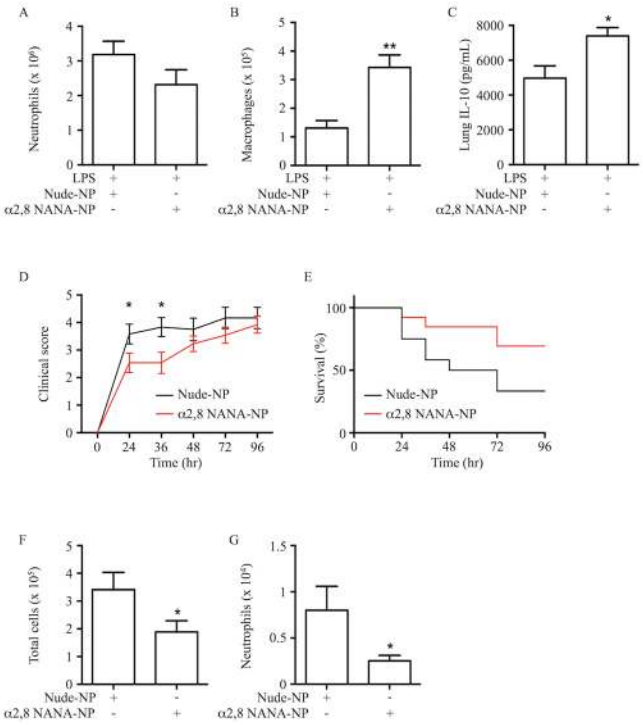

Fig. 4. α2,8 NANA-NP induces SHP-2 recruitment to Siglec-E to promote downstream anti-inflammatory responses

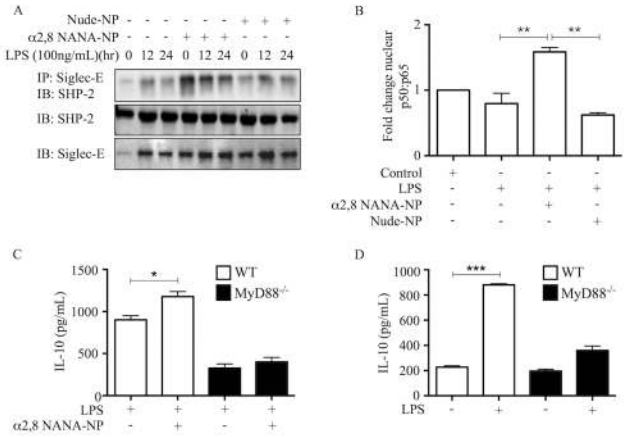

Fig. 5. Siglec-E is induced by IL-10 and the anti-inflammatory effects of α2,8 NANA-NP are IL-10 dependent

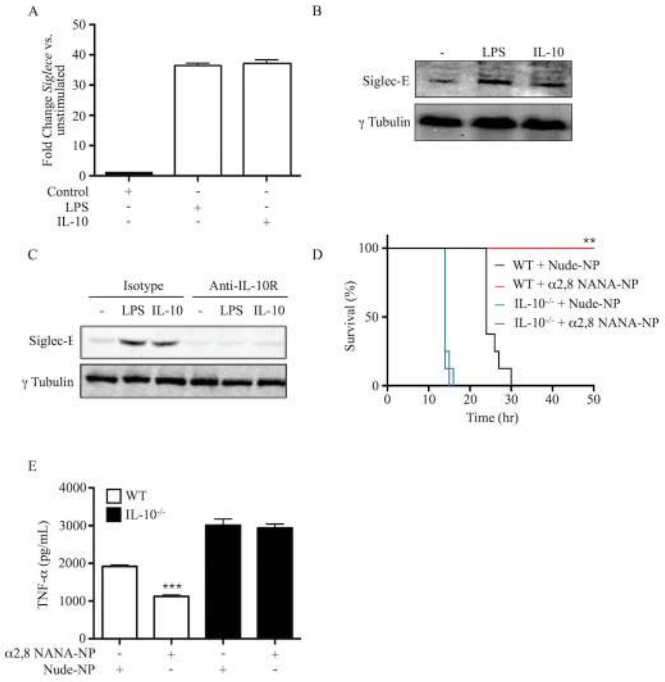

Fig. 6. α2,8 NANA-NP promotes anti-inflammatory effects in human cell assays

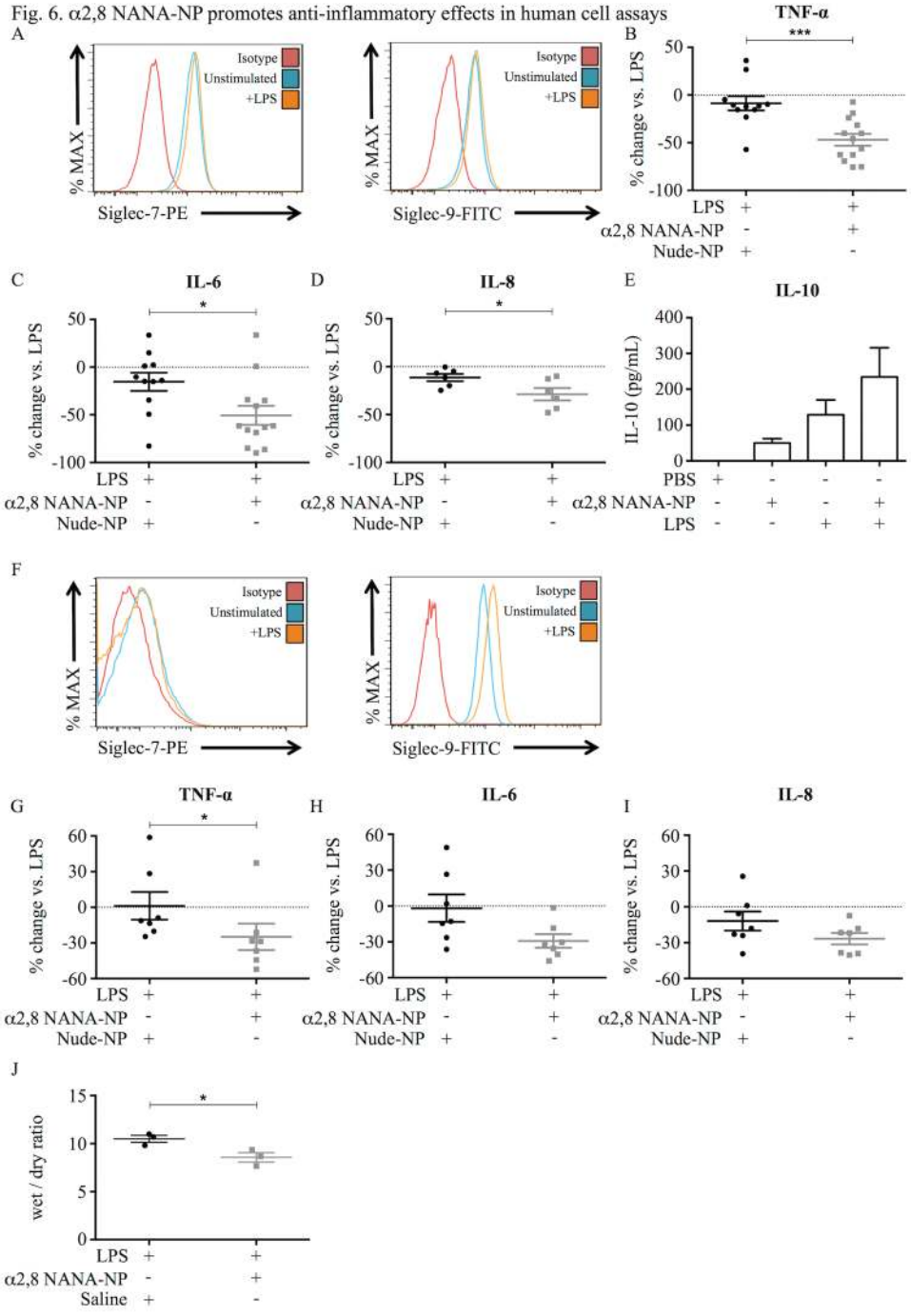

Supplementary methods:

Materials: PLGA (RG502H) was purchased from Evonik. Acetone, dichloromethane (DCM), poly(vinyl alcohol) (PVA; 87−89% hydrolyzed with a molecular weight of 13-23kDa), 2-(N-morpholino) ethanesulfonic acid (MES) hydrate, magnesium chloride hexahydrate ($MgCl_2$•$6H_2O$), N-Hydroxysuccinimide (NHS), rhodamine 6G, coumarin 6, purpald, sodium periodate and N-ethyl-N(3-dimethylaminopropyl) carbodiimide hydrochloride (EDC) were obtained from Sigma Aldrich. Di(α2→8) N-acetylneuraminic acid (α2,8 NANA) was purchased from Nacalai Tesque.

Preparation of PLGA nanoparticles: 20mg PLGA was dissolved in 300μL DCM and 500μL acetone and injected under moderate stirring into 3mL ice-cold solution containing 2.5% (w/v) PVA and 45% (w/v) $MgCl_2$•$6H_2O$ in pH 5 MES buffer. Both phases were then sonicated for 90sec on ice. An additional 5mL 2.5% (w/v) PVA in pH 5 MES buffer was added under moderate stirring. Samples were left stirring overnight to allow organic solvent evaporation. Nanoparticles were centrifuged at 100,000*g* for 10min at 4°C and washed three times with pH 5 MES buffer. Nanoparticle pellets were resuspended at 5mg PLGA/mL in pH 5 MES buffer prior to activation and conjugation.

Nanoparticle activation and conjugation: Nanoparticle surface activation was achieved through the addition of 100μL EDC (0.2M) and 100μL NHS (1.4M), both dissolved in pH 5 MES buffer, followed by incubation at room temperature for 1hr with moderate stirring. Nanoparticles were centrifuged at 100,000*g* for 10min at 4°C and resuspended at 1mg PLGA/mL in PBS. α2,8 NANA (100μg) was added to 1mL of activated nanoparticles and incubated at 4°C overnight. Finally, nanoparticles were centrifuged at 20,000*g* for 1hr at 10°C to remove excess, non-conjugated α2,8 NANA. Nanoparticle pellets were stored at -20°C and resuspended as required in the appropriate diluent.

Purpald assay for quantification of surface α2,8 NANA: 50μL of residual nanoparticle conjugation supernatant was incubated with 50μL sodium periodate (16mM) for 20min at room temperature in darkness. 50μL purpald reagent (136mM) was added and incubated as above. A further 50μL sodium periodate (64mM) was added and incubated for 20min as above before measurement of absorbance at 550nm and comparison with known standards of α2,8 NANA made up in Nude-NP supernatants.

Nanoparticle characterization: For scanning electron microscopy, α2,8 NANA-NP were mounted onto aluminium stubs using double-sided adhesive tape, coated with gold (Polaron E5150, Quorum Technologies) and visualized (Jeol 6500 FEG scanning electron microscope). Nanoparticle size and zeta potential were measured by dynamic light scattering and laser Doppler anemometry, respectively (Zetasizer Nano ZS system, Malvern instruments). For hyperspectral analysis, α2,8 NANA-NP and Nude-NP were adjusted to a concentration of 1mg/mL in distilled water. The samples were imaged using a

microscope fitted with the Cytoviva illumination setup (x100 magnification) and reflectance spectra were acquired in the wavelength range of 400-1,000nm at 2nm of spectral resolution. For ^{1}H nuclear magnetic resonance (NMR), samples were resuspended at 1mg/mL in deuterated dimethyl sulfoxide and analyzed using a Bruker Ultrashield 300MHz NMR spectrometer.

Binding of nanoparticles to Siglec-E recombinant protein: 1μg Siglec-E Fc recombinant protein (R&D Systems) was bound to Protein A/G agarose beads (Life technologies) and incubated ± 125μg/mL rhodamine 6G-loaded α2,8 NANA-NP or Nude-NP for 1hr. Beads were pelleted and washed by three centrifugations at 12,000*g* in 1mL PBS to remove non-bound nanoparticles. Binding of nanoparticles to Siglec-E Fc was measured by fluorescence at 560nm and expressed as fold-change in binding versus Siglec-E Fc alone.

Flow cytometric analyses of nanoparticle binding to macrophages and neutrophils: Peritoneal exudate cells from C57BL/6 mice treated with 1mg/kg LPS for 24hr were extracted and treated with 125μg/mL rhodamine 6G-loaded α2,8 NANA-NP or Nude-NP for 30min. Cells were washed with 3mL FACS Buffer at 500*g* for 5min at 4^{o}C. Cells were stained with antibodies against CD11b-APCcy7, F4/80-PEcy7, Ly6G-PerCP (EBiosciences) and Siglec-E-APC (R&D Systems). Rhodamine positivity was detected on FL-2 channel. In brief, cells were stained as per manufacturer's instructions for 30min on ice. Cells were washed once in FACS Buffer as above and resuspended in 200μL FACS Buffer. Cells were analyzed using a FACSCantoII flow cytometer and FACS DIVA (BD) and FlowJo software (Treestar). Representative plots are shown.

Histological analyses of lung, liver and kidney: Lungs, livers and kidneys were excised from three experimental conditions described in Fig. S5. Organs were fixed in 10% formalin prior to paraffin embedding. 6μm sections were stained using Harris haematoxylin and eosin (Fisher Scientific). In brief, slide sections were rinsed in two changes of clearene (Leica Biosystems) for 3min, rehydrated in 3min changes of ethanol (100%, 100%, 95%, 95% and 70%), followed by rinsing in distilled water for 5min. Sections were stained in haematoxylin for 6min and rinsed under tap water until clear. Slides were counterstained in eosin (30sec to 1min) and dehydrated through two changes of 95% ethanol, followed by two changes of 100% ethanol for 3min. Slide sections were rinsed in two changes of clearene for 3min and mounted with DPX mountant prior to imaging. Sections were imaged using a Leica DM5500 microscope (x10 magnification).

LDH quantification: Serum LDH levels were determined using commercially available kits (Roche or Sigma) in accordance with the manufacturer's instructions.

EVLP BAL fluid collection and processing: BAL fluid was collected at baseline and 4hr after LPS instillation. After the lung was rewarmed to 36^{o}C following perfusion and inflation of the lung, the right (RUL) or left (LUL) upper lobe was cannulated with a catheter and advanced until gentle resistance was

encountered. Following instillation of 125mL of 0.9% sodium chloride containing 5% high purity bovine serum albumin (Sigma Aldrich) into the RUL or LUL, lavage fluid was aspirated and centrifuged at 1000*g* for 5min at 4^{o}C. The acellular supernatants were stored at -80 ^{o}C.

Supplementary figure legends:

A

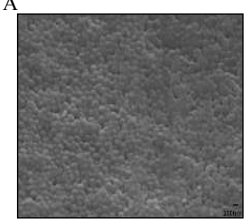

B

	Nude-NP	α2,8 NANA-NP
Size (nm)	151 ± 10	152 ± 13
Zeta potential (mV)	0.4 ± 0.4	0.3 ± 0.2
α2,8 NANA/ mg PLGA (μg)	0	15 ± 5

C

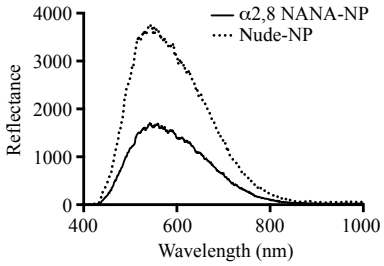

D

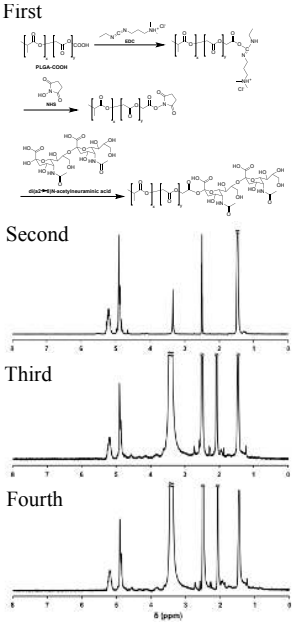

E

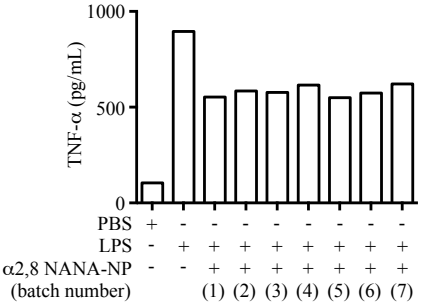

F

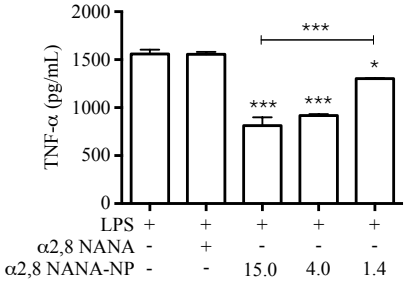

G

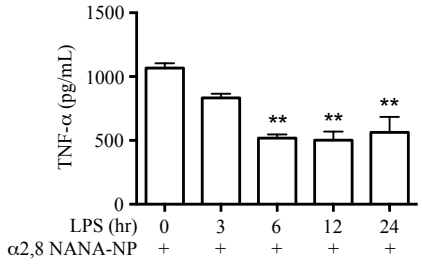

H

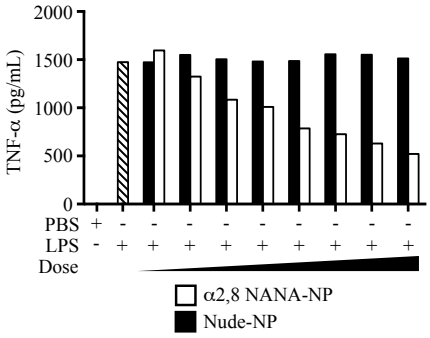

Fig. S1. Nanoparticle characterization. **(A)** Scanning electron microscopy image of freeze-dried nanoparticles. Scale bar = 100nm (representative image of n = 2 independent experiments). **(B)** Nanoparticle size and zeta potential were measured by dynamic light scattering and laser Doppler anemometry, respectively. Purpald assay was used to quantify the amount of α2,8 NANA on the nanoparticle surface. Data expressed as mean ± SD (n = 3 independent experiments). **(C)** Hyperspectral profiles of α2,8 NANA-NP and Nude-NP. α2,8 NANA-NP were associated with lower intensity scatter, whereas Nude-NP produced higher intensity scatter, indicating that the surface chemistries of α2,8 NANA-NP and Nude-NP were distinct from each other (n = 1 experiment). **(D)** Schematic of example proposed conjugation showing α2,8 NANA attachment to PLGA through free hydroxyls and confirmation of α2,8 NANA surface functionality by ^{1}H NMR (d_6-DMSO) spectroscopy. The spectrum for PLGA alone is shown in the second panel. The peaks at 5.21ppm and 1.47ppm correspond to the CH and CH_3 protons of the lactic acid monomer units, respectively. The peak at 4.90ppm relates to the CH_2 protons of the glycolic acid monomer units. The spectrum for Nude-NP (including EDC and NHS) is displayed in the third panel. The spectrum for the final product is presented in the fourth panel, following attachment of α2,8 NANA to Nude-NP via EDC/NHS chemistry. The appearance of a signal at approximately 1.90ppm corresponds to the methyl protons of the acetamido group of α2,8 NANA, thus confirming successful attachment of the targeting ligand to PLGA. Washing the sample with PBS appears to remove EDC and surplus α2,8 NANA not attached to PLGA, whilst there is also a reduction in the amount of NHS in the final product. Specifically, the peak at 2.58ppm, corresponding to the CH_2 protons of NHS, is more intense in the spectrum for Nude-NP. This peak is reduced by approximately 30% in the α2,8 NANA-NP spectrum (representative traces of three independent experiments). **(E)** C57BL/6 peritoneal macrophages were stimulated with 100ng/mL LPS ± 125μg/mL of seven independent preparations of α2,8 NANA-NP for 24hr. Supernatants were assayed for TNF-α by ELISA (n = 1 experiment). **(F)** C57BL/6 peritoneal macrophages were stimulated with 100ng/mL LPS ± 125μg/mL α2,8 NANA-NP conjugated with various amounts of α2,8 NANA or α2,8 NANA alone for 12hr. Supernatants were assayed for TNF-α by ELISA. Statistical significance was assessed by one way ANOVA with post-hoc Tukey test (*$p<0.05$, ***$p<0.001$, in comparison to LPS only). Data expressed as mean + SEM (n = 3 independent experiments in triplicate). **(G)** C57BL/6 BMDM were stimulated with 100ng/mL LPS ± 125μg/mL α2,8 NANA-NP for 0, 3, 6, 12 or 24hr. Supernatants were assayed for TNF-α by ELISA. Statistical significance was assessed by one way ANOVA with post-hoc Tukey test (**$p<0.01$, in comparison to 0hr). Data expressed as mean + SEM (n = 3 independent experiments in triplicate). **(H)** C57BL/6 peritoneal macrophages were stimulated with 100ng/mL LPS ± 2-fold serial dilutions of α2,8 NANA-NP or Nude-NP, ranging from 250μg/mL to 1.95μg/mL for 12hr. Supernatants were assayed for TNF-α by ELISA (n = 2 independent experiments in duplicate, with representative results from one experiment shown).

A

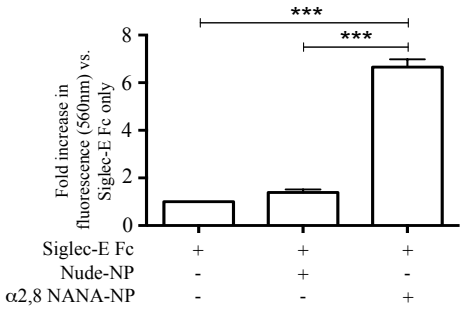

B

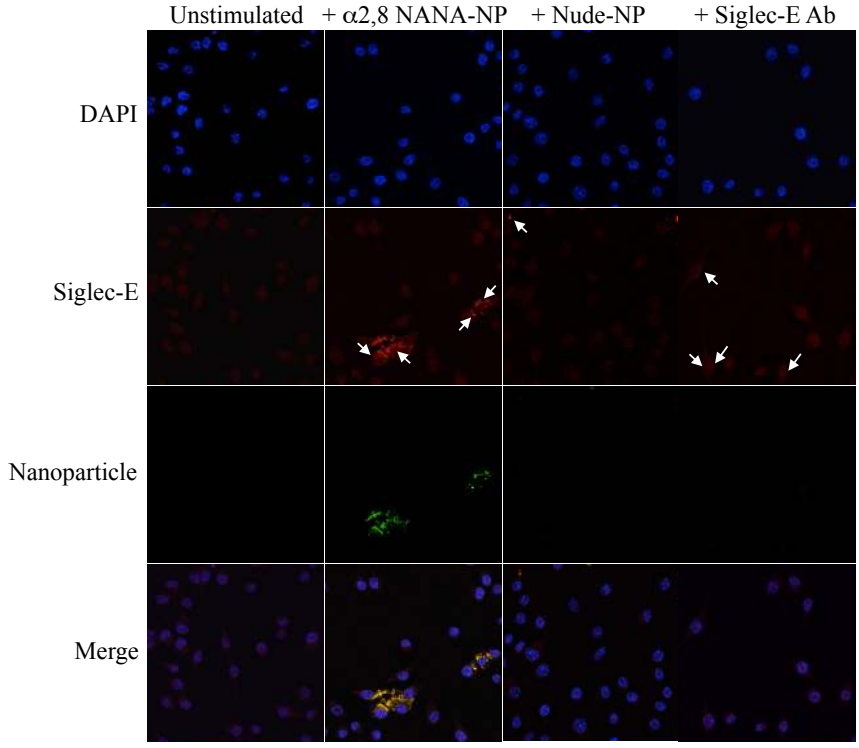

Fig. S2. α2,8 NANA-NP bind to Siglec-E and induce receptor clustering. **(A)** 1μg Siglec-E Fc was incubated with rhodamine 6G-loaded α2,8 NANA-NP or Nude-NP for 1hr. Binding of nanoparticles to Siglec-E Fc was measured by fluorescence and expressed as fold-change in binding versus Siglec-E Fc alone. Statistical significance was assessed by one way ANOVA with post-hoc Tukey test (***$p<0.001$). Data expressed as mean + SEM (n = 3 independent experiments in triplicate). **(B)** Confocal fluorescence microscopy images of RAW 264.7 cells treated with 125μg/mL rhodamine 6G-loaded α2,8 NANA-NP or Nude-NP (green) or 10μg/mL anti-Siglec-E antibody for 1hr. Cells were stained with anti-Siglec-E-APC (red) and ProLong Gold plus DAPI to visualize nuclei (blue). Arrows indicate clustering of Siglec-E (representative images of n = 2 independent experiments).

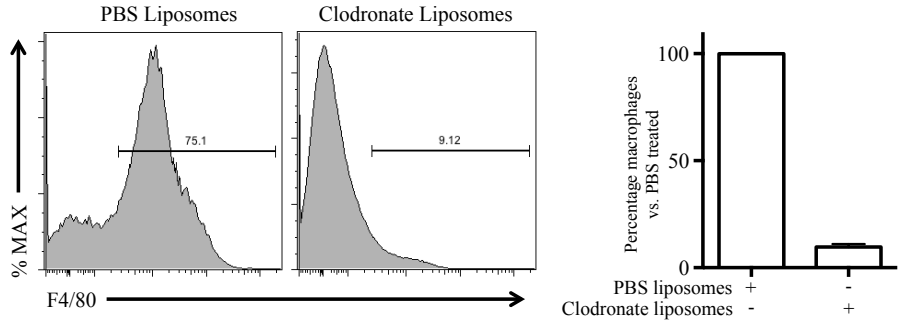

Fig. S3. Clodronate depletion of macrophages. C57BL/6 mice (n = 4 per group) were treated with PBS or clodronate liposomes 48hr and 24hr prior to extraction of peritoneal exudate. Cells were stained with F4/80-PEcy7 to discriminate macrophages and analyzed by flow cytometry. Representative histograms are shown. Bar graph represents percentage of macrophages present in clodronate group when compared to PBS liposome-treated controls. Data expressed as mean + SEM.

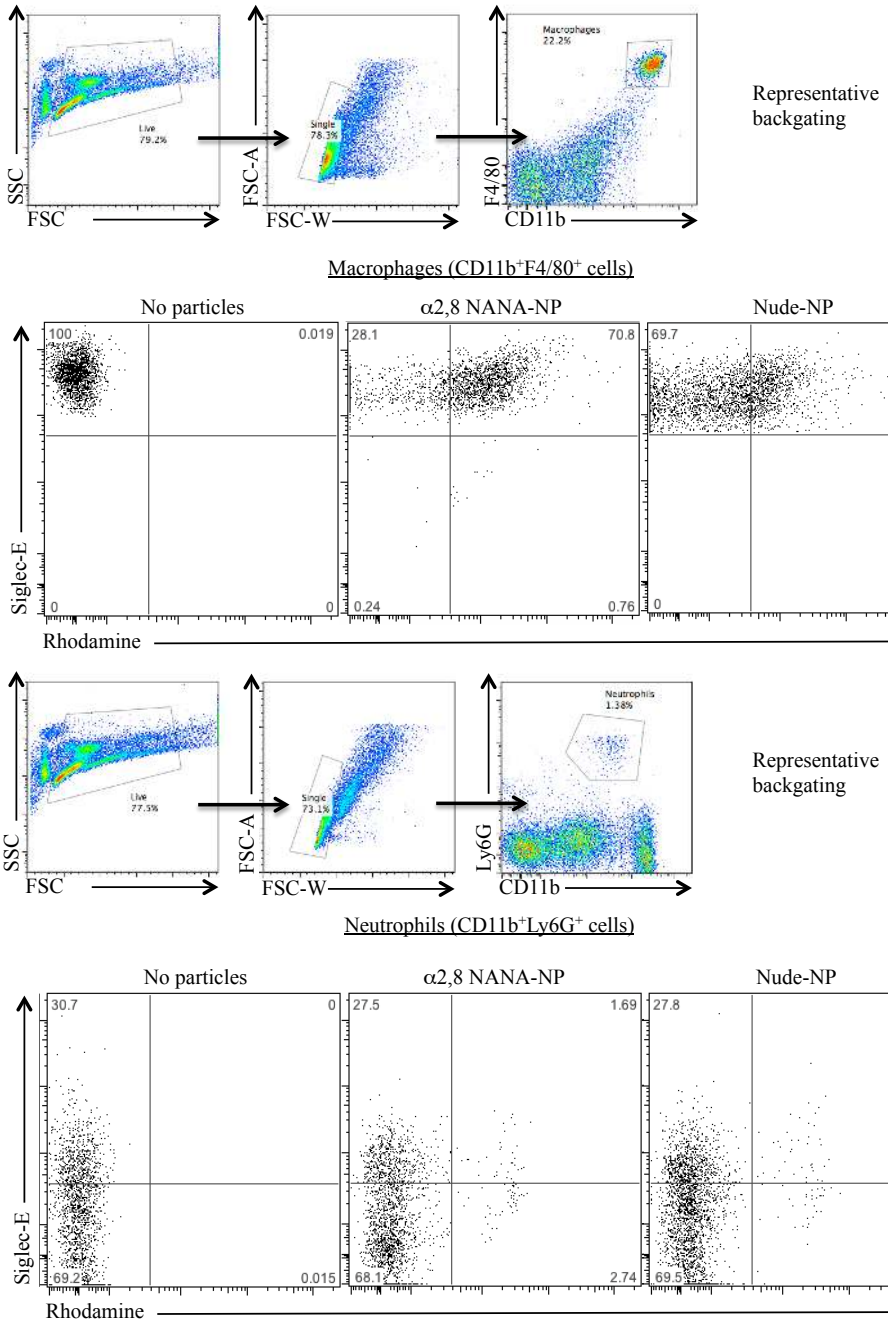

Fig. S4. Differential expression of Siglec-E and uptake of fluorescent α2,8 NANA-NP by macrophages and neutrophils. C57BL/6 peritoneal lavage cells were incubated with 125µg/mL rhodamine 6G-loaded α2,8 NANA-NP or Nude-NP for 30min. In addition to staining with Siglec-E-APC, cells were co-stained with CD11b-APCcy7 and F4/80-PEcy7 to discriminate macrophages or CD11b-APCcy7 and Ly6G-PerCP to discriminate neutrophils. Cells were analyzed by flow cytometry (representative plots of n = 2 independent experiments).

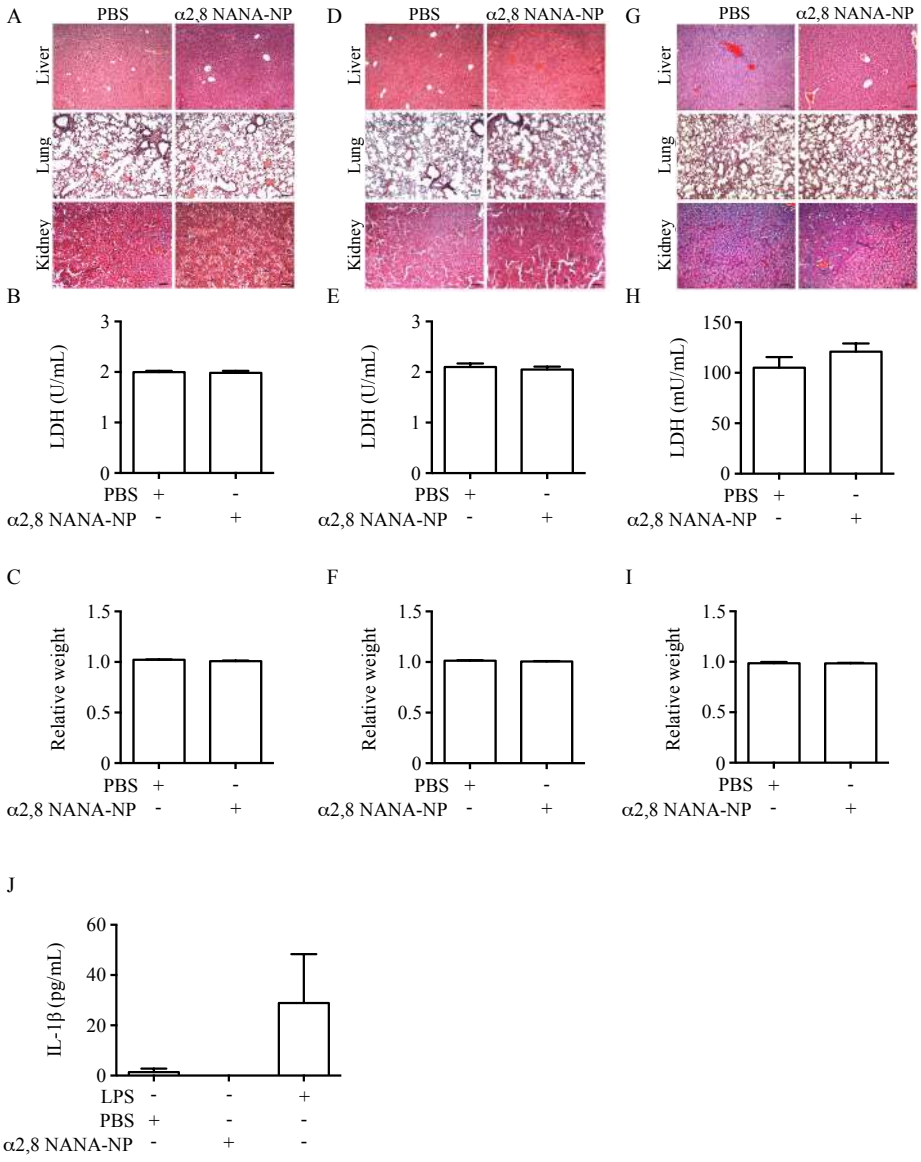
A
PBS
α2,8 NANA-NP
Liver
Lung
Kidney
D
PBS
α2,8 NANA-NP
Liver
Lung
Kidney
G
PBS
α2,8 NANA-NP
Liver
Lung
Kidney
B
LDH (U/mL)
3
2
1
0
PBS + -
α2,8 NANA-NP - +
E
LDH (U/mL)
3
2
1
0
PBS + -
α2,8 NANA-NP - +
H
LDH (mU/mL)
150
100
50
0
PBS + -
α2,8 NANA-NP - +
C
Relative weight
1.5
1.0
0.5
0
PBS + -
α2,8 NANA-NP - +
F
Relative weight
1.5
1.0
0.5
0
PBS + -
α2,8 NANA-NP - +
I
Relative weight
1.5
1.0
0.5
0
PBS + -
α2,8 NANA-NP - +
J
IL-1β (pg/mL)
60
40
20
0
LPS - - +
PBS + - -
α2,8 NANA-NP - + -

Fig. S5. α2,8 NANA-NP exhibit no toxicity in preclinical models. Nanoparticle toxicity was assessed in different experimental designs. **(A)** C57BL/6 mice (n = 3 per group) were treated with a single i.p. injection of PBS or 2mg α2,8 NANA-NP. At 28 days post-treatment, the liver, lungs and kidneys were excised for histological analysis. Representative images of H&E stained organ sections are shown. **(B)** Blood was collected by cardiac puncture and serum LDH levels were determined. Data expressed as mean + SEM. **(C)** Animal body weight was also assessed before and after treatment. Data presented as relative weight change post-treatment versus pre-treatment. Data expressed as mean + SEM. **(D-F)** In order to exclude toxicity and immune responses associated with repeated treatment regimes, C57BL/6 mice (n = 3 per group) were treated with weekly i.p. injections of PBS or 2mg α2,8 NANA-NP. At day 28, toxicology analysis was performed as in (A-C). **(G-I)** C57BL/6 mice (n = 3-5 per group) were treated with PBS or 1μg α2,8 NANA-NP i.t. At 24hr post-treatment, toxicology analysis was performed as in (A-C). **(J)** Primary human MDM (n = 3 donors) were stimulated with LPS or α2,8 NANA-NP. Supernatants were assayed for IL-1β by ELISA. Data expressed as mean + SEM.

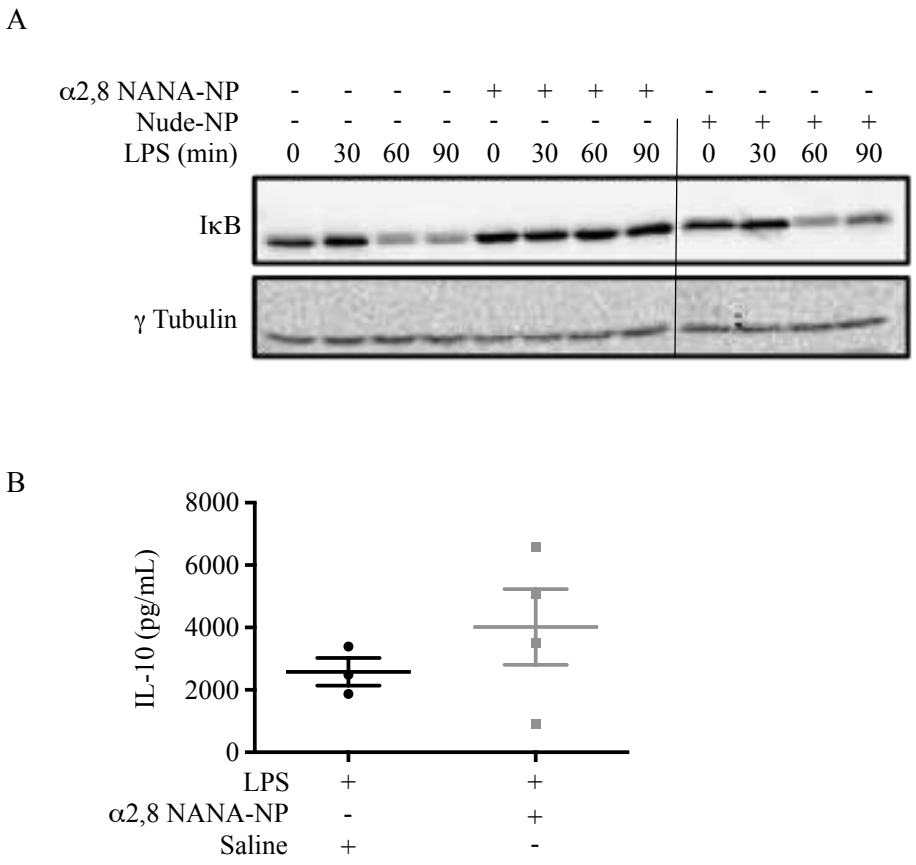

Fig. S6. α2,8 NANA-NP prevent IκB degradation in THP-1 cells and enhance IL-10 production in the EVLP model. **(A)** THP-1 cells were stimulated with 100ng/mL LPS ± 125μg/mL α2,8 NANA-NP or Nude-NP for 0-90min. Cells were lysed in RIPA prior to analysis of IκB and γ Tubulin protein expression by Western blot (representative image of n = 3 independent experiments). **(B)** Human lungs (n = 3-4 per group) were injured ex vivo by intrabronchial instillation of 6mg LPS. Lungs were treated simultaneously with saline or 5mg α2,8 NANA-NP, which were introduced into the perfusate in order to model systemic administration. At 4hr post-treatment, BAL fluid was collected. BAL fluid supernatants were assayed for IL-10 by ELISA. Data expressed as mean ± SEM.

A

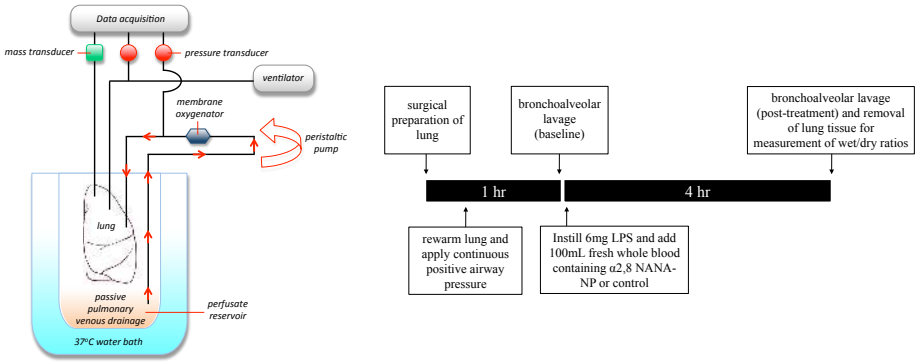

B

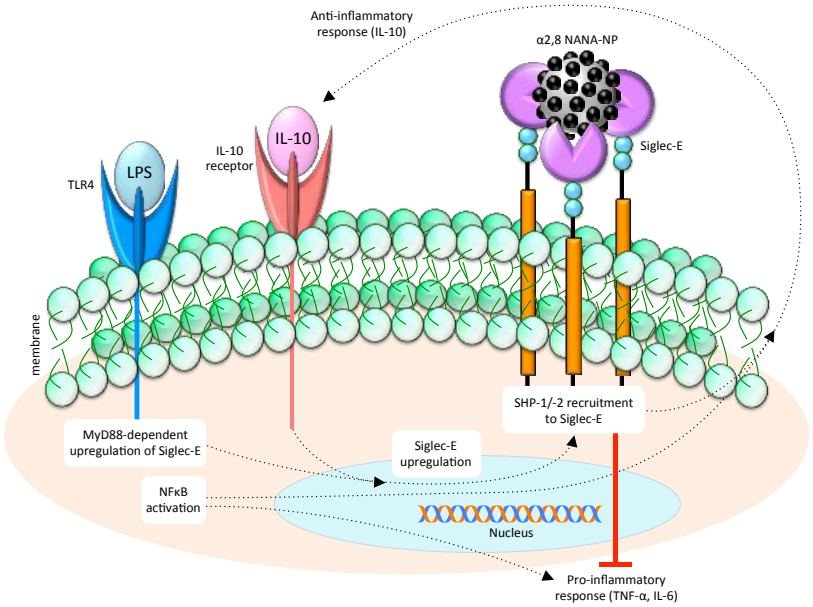

Fig. S7. Schematic of EVLP model and proposed mechanism of action of α2,8 NANA-NP. **(A)** Setup of EVLP model and associated treatment protocol. **(B)** Proposed anti-inflammatory action of α2,8 NANA-NP (NP not drawn to exact scale).